Chemistry and Physics of Lipids 219 (2019) 58–71

Contents lists available at ScienceDirect

Chemistry and Physics of Lipids

journal homepage: www.elsevier.com/locate/chemphyslip

Solid-state NMR structural investigations of peptide-based nanodiscs and of transmembrane helices in bicellar arrangements

Evgeniy S. Salnikov[a], Christopher Aisenbrey[a], G.M. Anantharamaiah[b], Burkhard Bechinger[a,*]

[a] Université de Strasbourg / CNRS, UMR7177, Institut de Chimie, 4, rue Blaise Pascal, 67070 Strasbourg, France
[b] Department of Medicine, Biochemistry & Molecular Genetics, University of Alabama at Birmingham, Birmingham, AL, 35294, USA

ARTICLE INFO

Keywords:
Oriented bilayer
Bicelle
Solid-state NMR
helix topology
Apo A-I mimetic
Rim structure
DIBMA polymer
DQA1 of MHC II
DQB1

ABSTRACT

The membrane topology of the peptide 18A, a derivative of apolipoprotein A-I, is investigated in structural detail. Apolipoprotein A-I is the dominant protein component of high density lipoproteins with important functions in cholesterol metabolism. 18A (Ac-DWLKA FYDKV AEKLK EAF- NH_2) was designed to mimic the structure of tandem domains of class A amphipathic helices and has served as a lead peptide for biomedical applications. At low peptide-to-lipid ratios 18A partitions into phosphatidylcholine membranes with helix topologies parallel to the membrane surface, an alignment that is maintained when disc-like bicelles form at higher peptide-to-lipid ratios. Notably, the bicelles interact cooperatively with the magnetic field of the NMR spectrometer, thus the bilayer normal is oriented perpendicular to the magnetic field direction. A set of peptides that totals four ^{15}N or ^{2}H labelled positions of 18A allowed the accurate analysis of tilt and azimuthal angles relative to the membrane surface under different conditions. The topology agrees with a double belt arrangement forming a rim that covers the hydrophobic fatty acyl chains of the bicelles. In another set of experiments, it was shown that POPC nanodiscs prepared in the presence of diisobutylene/maleic acid (DIBMA) polymers can also be made to align in the magnetic field. Finally, the transmembrane domains of the DQ alpha-1 and DQ beta-1 subunits of the major histocomptability complex (MHC) class II have been prepared and reconstituted into magnetically oriented bicelles for NMR structural analysis.

1. Introduction

1.1. High density lipoproteins and apolipoprotein A-I in cardiovascular disease

High density lipoproteins (HDL) exert protective effects on the artery wall (Ashby et al., 1998; Assmann and Gotto, 2004; Cockerill et al., 2001). Administration of apolipoprotein A-I and HDL in animal models of atherosclerosis show that HDL and apolipoprotein A-I exhibit anti-atherogenic properties (Rubin et al., 1991). However, HDL can also be functionally defective which led several investigators to explore new therapeutic targets for the modulation of HDL function (Kontush and Chapman, 2006). This is supported by the fact that treatment of HDL with apolipoprotein A-I mimetic peptides or administration of the apolipoprotein A-I mimetic peptides in animal models of atherosclerosis converts pro-inflammatory into an anti-inflammatory HDLcomplex (cf. below).

Recently, increasing attention has been focused on pharmacological treatments that elevate HDL cholesterol in order to prevent coronary artery disease and coronary events (Newton and Krause, 2002). A pilot clinical trial of infusion of a recombinant apolipoprotein A-I $_{Milano}$-phospholipid complex showed significant and rapid regression of atherosclerosis in human coronary arteries (Nissen et al., 2003) and has attracted further interest in recombinant HDL therapy. Apolipoprotein A-I $_{Milano}$-phospholipid complexes also produced a rapid reversal of endothelial dysfunction in apolipoprotein E null mice (Kaul et al., 2004). However, the practicality of this form of therapy, due to high costs and requirement of infusion, has yet to be determined. Thus, there

Abbreviations: CHAPS, 3-[(3-**ch**olamidopropyl)dimethyl**a**mmonio]-1-**p**ropane**s**ulfonate; CHAPSO, 3-[(3-cholamidopropyl)dimethylammonio]-2-hydroxy-1-propanesulfonate; DIBMA, diisobutylene/maleic acid copolymer; DHPC, 1,2-di-hexanoyl-*sn*-glycero-3-phosphocholine; DMPC, 1,2-di-myristoyl-*sn*-glycero-3-phosphocholine; HDL, high density lipoprotein; HFIP, hexafluoro isopropanol; LWHH, line width at half height; MAS, magic angle spinning; MSP, membrane scaffolding protein; NMR, nuclear magnetic resonance; PC, phosphatidylcholine; POPC, 1-palmitoyl-2-oleoyl-*sn*-glycero-3-phosphocholine; SMA, styrene maleic acid copolymer; 14A, peptide with the sequence Ac-DYLKA FYDKL KEAF- NH_2; 18A, peptide with the sequence Ac-DWLKA FYDKV AEKLK EAF- NH_2

* Corresponding author at: Faculté de chimie, Institut le Bel, 4, rue Blaise Pascal, 67070, Strasbourg, France.
E-mail address: bechinge@unistra.fr (B. Bechinger).

https://doi.org/10.1016/j.chemphyslip.2019.01.012
Received 26 October 2018; Received in revised form 29 January 2019; Accepted 29 January 2019
Available online 31 January 2019
0009-3084/

is a growing interest in alternative modes of HDL therapy.

Apolipoprotein A-I is considered an important element in defining the size and shape of HDL particles (Gogonea, 2015). The structure of apolipoprotein A-I has been described by a molten globular state, adopting helix secondary structure in an environment-dependent manner (Gogonea, 2015) similar to many other amphipathic peptides (Bechinger and Aisenbrey, 2012). Therefore, it has not been possible to determine the high-resolution structures of full length apolipoprotein A-I either in the absence or in the presence of lipids (Gogonea, 2015; Phillips, 2013). However, deuterium exchange experiments revealed the outlines of helical domains when associated with lipids while an X-ray structure of a truncated apolipoprotein A-I (residues 44-243) in the lipid-free state in combination with chemical cross linking reveals a horseshoe shaped continuous helix with proline kinks (Phillips, 2013).

Taking apolipoprotein A-I as a template, shortened sequences have been engineered to be used as membrane scaffolding protein (MSP). These constructs initially consisted of only 10 amphipathic helices from the apolipoprotein A-I structure (Schuler et al., 2013), but new shapes are continuously developed and analyzed because they have shown to be useful for structural analysis of membrane proteins (Bibow et al., 2017; Hagn et al., 2018).

1.2. Apolipoprotein mimetic peptides

A rapidly developing area in the field of HDL therapy is the design of apolipoprotein mimetic peptides. Synthetic apolipoprotein A-I mimetics that are designed based on the lipid-associating domains of apolipoprotein A-I have been shown to stimulate an increase in HDL concentration and/or PON-1, an antioxidant enzyme capable of hydrolyzing oxidized phospholipids that are associated with a decrease in atheroma formation in apolipoprotein E null and LDL-receptor null mice on Western diet (Navab et al., 2002, 2004). Knowledge obtained by the studies of peptide analogs, which have yielded unique and, in several cases, unexpected results, have enabled the understanding of apolipoprotein A-I structure and function as well as HDL function.

It was hypothesized that if the amphipathic helical structure is responsible for solubilizing lipids, then, even small peptide molecules that can form amphipathic helices should act as peptide detergents to solubilize phospholipids. Computer analysis revealed that most of the helices in apolipoproteins showed a particular pattern of amino acid distribution, in which basic residues (Arg and Lys) are located at the polar - nonpolar interface and negatively charged residues at the center of the polar face. Such amphipathic helices were called class A helices (Segrest et al., 1974).

The first peptide designed to mimic the amphipathic helical domains of apolipoprotein A-I was 18A, which does not possess sequence homology to any of the exchangeable apolipoproteins (Anatharamaiah et al., 1985). This peptide was able to interact with 1,2-dimyristoyl-*sn*-glycero-3-phosphocholine (DMPC) to form discoidal structures that were similar in size and shape to those formed by apolipoprotein A-I :DMPC (Anantharamaiah and Goldberg, 2015). Based on these observations and the ability of these complexes to efflux cholesterol from cells and activation of lecithin:cholesterol acyltransferase (LCAT), they were termed the apolipoprotein A-I mimetic peptides (Anantharamaiah, 1986; Anantharamaiah et al., 1985). Related to apolipoprotein A-I and HDL, 18A and its analogs exhibit anti-inflammatory properties and ameliorate several lipid-mediated inflammatory diseases when tested in animal models of diseases (Anantharamaiah and Goldberg, 2015). The 18A analogue D-4 F (synthesized using all D-amino acids) is orally active and improves HDL function (Dunbar et al., 2017). A shortened version of 18A forms bicellar structures of related properties (Anantharamaiah and Goldberg, 2015; Anantharamaiah et al., 2007). Recently, the 14A peptide was obtained by deleting one helical pitch from 18A and has been investigated by solid-state NMR spectroscopy, a technique also used here, indicating a double belt helical arrangement of 14A forming the rim of the corresponding bicelle (Salnikov et al., 2018). Here we present more detailed data on the parent peptide 18A in order to further test if the previous models are more generally applicable to other amphipathic sequences and to test if the published ideas on apolipoprotein structures can be consolidated.

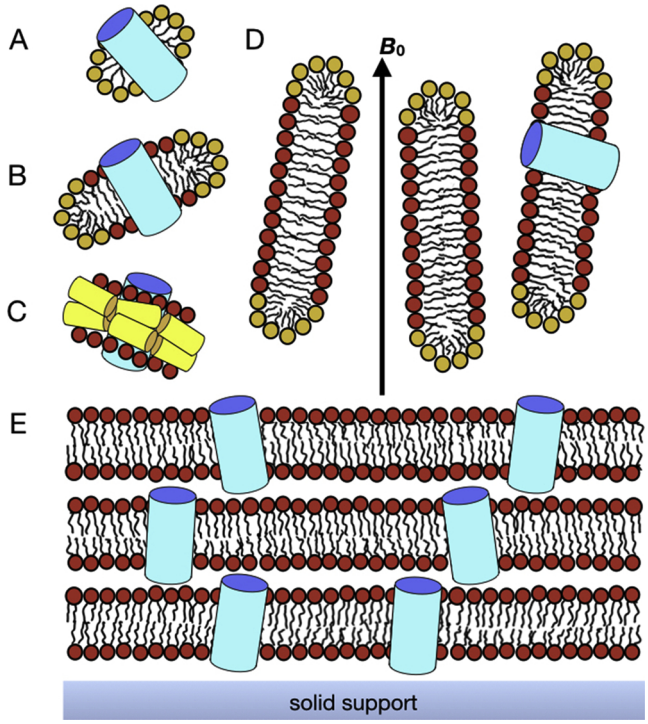

Fig. 1. Supramolecular membrane assemblies used in structural investigations. **A.** Micelle **B.** Isotropic bicelle with a high content of short chain lipids. **C.** The membrane scaffolding protein forms the rim around a lipid bilayer of about 100 lipids and results in nanodiscs of defined size. A double belt arrangement is shown. **D.** Large bicelles made of short and long chain phospholipids. At the correct lipid composition, temperature and hydration these align in the magnetic field. **E.** Stacks of oriented bilayers on a solid support such as glass plates or plastic sheets. For solid-state NMR studies the membrane normal is usually aligned parallel to the magnetic field of the spectrometer.

1.3. Membrane model systems and the use of bicelles in structural studies

In order to study the structure, dynamics, topology and interactions of membrane polypeptides, liquid crystalline bilayers closely matching their physiological environment are used and a variety of NMR spectroscopic approaches have been developed (Baker and Baldus, 2014; Kim et al., 2015; Xu et al., 2010). Continuous progress in multi-dimensional solution NMR spectroscopy has opened applications of the technique to biomolecular complexes of up to 900 kDa in size (Fiaux et al., 2002). Because this technique requires that the systems reorient fast on the NMR time scale, small membrane-mimetic supramolecular complexes such as micelles or isotropic bicelles have been introduced (Fig. 1A–C) (Frey et al., 2017). On the other hand, solid-state NMR approaches have been developed for the study of the structure, topology and dynamics of polypeptides in extended liquid crystalline lipid bilayers (Baker and Baldus, 2014; Bechinger et al., 2011; Kim et al., 2015; Xu et al., 2010). Because of the anisotropy of most NMR interactions, the lines are broadened in the solid state. Fast magic angle sample spinning of membrane pellets and vesicles is applied, which averages dipolar interactions and chemical shift anisotropies (Baker and Baldus, 2014; Das et al., 2015; Eddy et al., 2015; Ladizhansky, 2017; Lakomek et al., 2017; Lalli et al., 2017; Retel et al., 2017). An alternative solid-state NMR approach is based on samples that are uniaxially aligned relative to the magnetic field direction thereby introducing spectral resolution, at the same time angular information is

obtained (Bechinger et al., 2011; Das et al., 2015; Gopinath et al., 2015). These investigations require the preparation of lipid bilayer stacks on solid supports (Aisenbrey et al., 2013) or polypeptide reconstitution in bicelles / large nanodiscs, that interact with and orient relative to the large magnetic field of the NMR spectrometer (Das et al., 2015; Gopinath et al., 2015; Prosser et al., 2006; Ravula et al., 2018; Salnikov et al., 2018) (Fig. 1D,E).

In the context of this special issue on lipid bicelles three complementary topics from our laboratory will be discussed. In a first step, the structural details on the structure and dynamics of these supramolecular assemblies have been obtained by oriented solid-state NMR and CD spectroscopies. Furthermore, ongoing work on how bicelles can be used for solid-state NMR structural investigations and possible future developments will be presented.

First of all, the general features of such supramolecular structures are of interest. Bicelles are made of patches of bilayers that, depending on the detailed composition, vary in size (typically tens of nanometers) and are thought to represent many essential features of biological membranes. Because they do not form closed structures like vesicles, it is necessary to screen the hydrophobic fatty acyl chains of the bilayer lipids by rim-forming molecules. Rims can be made of detergents such as CHAPS/O (Nolandt et al., 2012; Vold and Prosser, 1996), with short chain phospholipids such as dihepta- or dihexa-PC (Das et al., 2015; Durr et al., 2012; Marcotte and Auger, 2005; Prosser et al., 2006; Wang et al., 2018; Warschawski et al., 2011), styrene maleic acid copolymers (SMA) (Ramadugu et al., 2017; Ravula et al., 2017b,c) or of polypeptides (Bechinger, 2005; Salnikov et al., 2018; Wolf et al., 2017). Bicelles prepared with detergents or short-chain lipids were the first systems investigated by NMR spectroscopy and have been studied quite extensively (Vold and Prosser, 1996). It has been determined that the ratio between rim- and bilayer-forming short and long chain phospholipids (q-ratio) has a profound influence on the size of the supramolecular complex. Micellar, bicellar and extended membranes are observed depending on q-ratio, water content and temperature. By adjusting these conditions, the bicellar phases can be made to align with the membrane normal perpendicular to the magnetic field of the NMR spectrometer (B_o) (Loudet et al., 2010; Marcotte and Auger, 2005). Preliminary investigations show that bicelles made from other rim-forming molecules such as scaffolding proteins (MSP) (Bibow et al., 2017; Hagn et al., 2018; Schuler et al., 2013), polypeptides (Bechinger, 2005; Salnikov et al., 2018; Wolf et al., 2017) or polymers (Bersch et al., 2017; Ravula et al., 2018) seem to follow related phase behavior.

1.4. Rims made of polypeptides

MSPs have been designed for structural investigations using nanodiscs of defined size (Bibow et al., 2017; Hagn et al., 2018; Schuler et al., 2013). Different MSP variants have been prepared which form nanodiscs about 10–17 nm in diameter encompassing 120–650 phosphatidylcholine lipids (Schuler et al., 2013). Thus MSP, being a recombinant apolipoprotein A-I protein, is thought to wrap around the rim of a lipid bilayer in a double belt arrangement, assuring a homogenous, stable and reproducible geometry (Schuler et al., 2013). It would therefore be of high interest to evaluate in detail how the rims of such discoidal supramolecular structures form (Fig. 1C).

In agreement with the molten globular nature of apolipoprotein A-I (Gogonea, 2015) MSPs seem to consist of a loose string of helical segments punctuated by Pro and Gly residues, where the size of the resulting nanodisc is a function of their number and length (Schuler et al., 2013). Whereas the covalent linkage between MSP helices defines the size of the resulting nanodisc this is not the case for bicelles made of 18A or other amphipathic peptides. In the latter cases the ratio of peptide-to-lipid has a profound influence on the geometry of the nanostructure (Wolf et al., 2017), demonstrating the importance of adjusting the ratio of peptide/short chain to long chain lipids for this type of bicelle (Marcotte and Auger, 2005).

Unique examples for peptide-based nanodiscs are mixtures of lipids with 14A (Salnikov et al., 2018), 18A and 22A (Zhang et al., 2016), which are mimetics of the biomedically important apolipoproteins. Nanodiscs from these polypeptides are more easily accessible to NMR structural investigations than the full-length apolipoprotein A-I (Park et al., 2011). At the same time, these complexes maintain important properties of the parent protein (Anantharamaiah, 1986). They also reflect some of the essential structural arrangements of the full protein. Whereas cytochrome C has recently been studied by multidimensional solution NMR spectroscopy in 22A nanodiscs, small enough to move isotropically (Ravula et al., 2017a; Zhang et al., 2016), the 14A peptide structure, topology and interactions have recently been determined in the context of planar lipid membranes and of bicellar environments (Salnikov et al., 2018). Here we investigated the supramolecular interactions and topology of 18A, a peptide derived from the apolipoprotein A-I secondary structure (Anatharamaiah et al., 1985). This peptide has been studied extensively in biological assays (Anantharamaiah et al., 1985; Epand et al., 1987; Jorgensen et al., 1989) and has become the template for the design of several analogs.

Static oriented solid-state NMR spectroscopy was used to determine the topologies of the 18A helix relative to the normal of either extended supported lipid bilayers, or of peptide-based nanodiscs that magnetically orient in the field of the NMR spectrometer. Information from ^{15}N and/or ^{2}H labelled 18A reconstituted into bilayers or discs provides the angular restraints to determine the peptide topology relative to the membrane normal. Simultaneously the phospholipid alignment is also monitored by ^{31}P solid-state NMR spectroscopy. From such oriented samples, the anisotropic ^{15}N chemical shifts and ^{2}H quadrupolar splittings provide angular information on helix topology and dynamics of the labeled sites and ultimately 18A (Bechinger et al., 2011). Comparison with the 14A structure and alignment within lipid bilayers sheds light on the supramolecular organization of amphiphiles that help shape native lipoproteins; furthermore, designed peptides have potential medical applications (Anantharamaiah and Goldberg, 2015).

As an example of how magnetically oriented bicelles can contribute to the structural investigation of membrane proteins, we investigated a sequence of the major histocompatibility complex (MHC) class II. The DQ alpha-1 (DQA1) domain of this complex assembles with the beta chain to form a transmembrane heterodimer through GXXXG-mediated protein-protein (Russ and Engelman, 2000) and protein-lipid interaction motifs (Contreras et al., 2012). Notably, an amino acid sequence promoting highly specific interactions with sphingomyelin carrying a C-18 chain was identified within DQA1 and many other proteins that localize membrane proteins to the plasma membrane and to organelles of the secretory pathway (Bjorkholm et al., 2014). Because MHC class II proteins fulfill important functions in adaptive immunity and are associated with many autoimmune diseases such as type I diabetes and chronic inflammatory conditions (Tsai and Santamaria, 2013), we aim at a structural analysis of the DQA1 and DQB1 transmembrane domains and their interactions. As a first step the polypeptides were synthesized carrying a ^{15}N label at a single site, reconstituted into bicelles that orient in the magnetic field of the NMR spectrometer and the spectra recorded.

Finally, styrene/maleic acid (SMA) copolymers have been developed during recent years as an alternative means to extract membrane proteins and for NMR structural investigations (Bersch et al., 2017; Radoicic et al., 2018; Ravula et al., 2018). Such systems allow for the direct extraction of membrane proteins without detergents. However, because of the presence of aromatic moieties, the SMA copolymers as well as the MSP show strong absorption in the UV range hampering optical investigations of the nanodisc inserted membrane proteins (Oluwole et al., 2017b). More recently diisobutylene/maleic acid (DIBMA) has been shown to have several advantages for membrane extraction because it has only a mild effect on the fatty acyl chains, does not interfere with optical spectroscopy in the UV range and exhibits better solubility in the presence of divalent cations (Oluwole et al.,

Table 1
Amino acid sequences of peptides investigated in this paper.

Peptide 18A Ac-DWLKA FYDKV AEKLK EAF- NH_2[^{15}N-Phe6,$^{2}H_3$C-Ala5]
Ac-DWLKA FYDKV AEKLK EAF- NH_2[^{15}N-Val10,$^{2}H_3$C-Ala11]
Peptide 14A: Ac-DYLKA FYDKL KEAF-NH_2 (Salnikov et al., 2018)
Peptide 22A: PVLDLFRELLNELLEALKQKLK (Zhang et al., 2016)
DQA1-TMD: KK TETVV CALGL SVGLV GIVVG TVFII RGLRS KK
(amino acids 215-244; uniprot P01909)
DQB1-TMD: KK QSKML SGIGG FVLGL IFLGL GLIIH HRSQK K
(amino acids 228-257; uniprot P01920)

2017a, b). Here we tested the magnetic alignment properties of DIBMA-based nanodiscs.

2. Materials & methods

2.1. Peptides and lipids

1, 2-dimyristoyl-*sn*-glycero-3-phosphocholine (DMPC) was from Avanti Polar Lipids (Alabaster, AL). ^{2}H-depleted water (< 1 ppm) from Sigma-Aldrich, France.

The amino acid sequences of peptides studied in this paper and the DIBMA structure are shown in Table 1.

The transmembrane domains of DQA1 and DQB1 are underlined. For better solubility and handling two lysines were added at each terminus of DQA1 and the N-terminus of DQB1 as well as a second K to the C-terminus of the latter.

The peptides were synthesized by solid-phase peptide synthesis using a Millipore 9050 automatic peptide synthesizer and Fmoc-chemistry. At selected positions Fmoc-protected amino acid precursors carrying stable ^{15}N or ^{2}H isotopes were inserted (Euriso-top, Paris, France or Isotec® Sigma-Aldich St Quentin Fallavier, France). The peptides were purified by reverse phase HPLC (Gilson, Villiers-le-Bel, France) using an acetonitrile/water gradient applied to a preparative C-18 column (Luna, C18-300Å-5 µm, Phenomenex, Le Pecq, France) or a semipreparative C-4 column (Nucleosil C4-300Å-7 µm, Macherey-Nagel, Düren, Germany). The peptide identity and purity (> 90%) were checked by analytical HPLC and MALDI mass spectrometry (MALDI-TOF Autoflex, Bruker Daltonics, Bremen, Germany) before lyophilization and storage at −20 °C.

2.2. Preparation of samples for oriented solid-state NMR spectroscopy

The 18A samples were prepared, investigated by solid-state NMR and analyzed in an analogous manner as described previously for 14A (Salnikov et al., 2018) and detailed with illustrations in (Aisenbrey et al., 2013). When calculating molar ratios the MW determined in mass spectrometric analysis were used thereby ignoring the counter ions. The methods were adjusted for the DQA1 and DIBMA investigations and are detailed here.

For reconstitution of DQA1 or DQB1 into bicelles, 1 mg of peptide in HFIP/water (100 µl/100 µl) was added to a solution of DMPC/DHPC (11 mg/2.25 mg; q = 3.2) lipids in HFIP (400 µl) in four steps of 50 µl each. After each step, the sample was vortexed and the solvent partially evaporated to reduce the volume to 300 µl. Thereafter, the lipid/peptide mixture was dried under a stream of nitrogen and the resulting films were placed under vacuum for 2 days to remove the remaining organic solvent. An appropriate amount of ^{2}H-depleted water was added to the dry film to reach a total lipid content of 28% (w/v). Four cycles of vortexing, heating to 45 °C and chilling on ice (0 °C) were performed to obtain bicelle samples that are fluid at 0 °C and viscous at 45 °C.

The DIBMA solution (Sokalan ® CP9, BASF, Ludwigshafen, Germany) was a generous gift from the laboratory of Sandro Keller at the Technische Universität Kaiserslautern (TUK). The DIBMA solution was precipitated by slow addition of 1 M HCl. The precipitate was centrifuged and washed at least 5 times with miliQ water and lyophilized. Lipid and DIBMA powder were mixed in dichloromethane with the help of a sonication bath. The dichloromethane was removed first with a stream of nitrogen and thereafter by exposure to high vacuum overnight. Buffer was added, the pH was verified with pH paper (Macherey und Nagel, Düren, Germany) and readjusted using 1 M NaOH. The DIBMA samples were centrifuged into a 2.5 mm MAS rotor.

2.3. Solid-state NMR spectroscopy

Proton-decoupled ^{31}P solid-state NMR spectra were typically acquired at 121.577 MHz on a Bruker Avance wide-bore 300 NMR spectrometer equipped with a double-resonance flat-coil probe (Rheinstetten, Germany). The temperature was set to 37 °C. Spectra were recorded with a Hahn-echo pulse sequence (Rance and Byrd, 1983) using a π/2 pulse of 5 µs, a spectral width of 100 kHz, an echo delay of 40 µs, an acquisition time of 10.2 ms, and a recycle delay of 3 s. External 85% H_3PO_4 was set to 0 ppm.

Proton-decoupled ^{31}P solid-state NMR spectra of the DIBMA samples in an MAS rotor were acquired on a Bruker Avance wide-bore 750 NMR spectrometer (Rheinstetten, Germany) using a single pulse experiment with a π/2 pulse of 3 µs.

To record ^{2}H solid-state NMR spectra of $^{2}H_3$-alanine-labelled 18A a quadrupolar echo pulse sequence was used (Davis et al., 1976) with the following parameters: π/2 pulse 5 µs, echo delay 50 µs, acquisition time 25.6 ms, and recycle delay 1.5 s, temperature 37 °C. A dwell time of 0.5 µs was used which allows to find the echo top with high precision (spectral filters at 125 kHz). An exponential apodization function corresponding to a line broadening of 300 Hz was applied before Fourier transformation. $^{2}H_2O$ set to 0 Hz was used as a reference.

Proton-decoupled ^{15}N cross-polarization (CP) spectra of static samples aligned on glass plates were recorded at 30.43 MHz on a Bruker Avance wide bore 300-MHz NMR spectrometer using a double-resonance flat-coil probe (Bechinger and Opella, 1991) and an adiabatic CP pulse sequence (Hediger et al., 1994). The spectral width, acquisition time, CP contact time, and recycle delay time were 25 kHz, 10.2 ms, 0.6 ms, and 3 s, respectively. The ^{1}H π/2 pulse and SPINAL-64 heteronuclear decoupling field strengths were 35 kHz (Fung et al., 2000). The temperature was set to 37 °C, i.e. well above the gel-to-liquid phase transition of DMPC (T_c = 23 °C). Before Fourier transformation a 50 Hz exponential line-broadening was applied. $^{15}NH_4Cl$ at 40.0 ppm was used as an external reference (Bertani et al., 2014). The ^{15}N spectra of the bicelle samples were measured with a static e-free probe at 17.6 T (Bruker Biospin, Rheinstetten, Germany).

2.4. Orientation restraints from the solid-state NMR spectra

To calculate the peptide alignments relative to the membrane that agree with the experimental spectra, a coordinate system was defined with the tilt angle being the angle between the helix long axis and the membrane normal, and an azimuthal angle between the membrane normal and a plane through the hydrophobic/hydrophilic interface of the peptide helical wheel projection (see Fig. 5E for angle definitions). The ^{15}N chemical shift main tensor elements were 56 ppm, 81 ppm and 223 ppm (Salnikov et al., 2009). The reference quadrupolar splitting at room temperature was 74 kHz for the alanine $^{2}H_3$C-group (Batchelder et al., 1983). A variety of α-helical conformations were tested as indicated in the text. The tilt and pitch angles were successively changed (50 × 50 steps) and the corresponding ^{15}N chemical shift and quadrupolar splitting calculated (Michalek et al., 2013). The standard deviation of a Gaussian line shape provides the measure for orientational heterogeneity during the restriction analysis, where two models were tested. In the first the peptide was static whereas in the second independent wobbling (10° Gaussian distribution) and azimuthal fluctuations around the helix long axis (18°) were taken into consideration by averaging the resonance values on the ensemble of orientations with

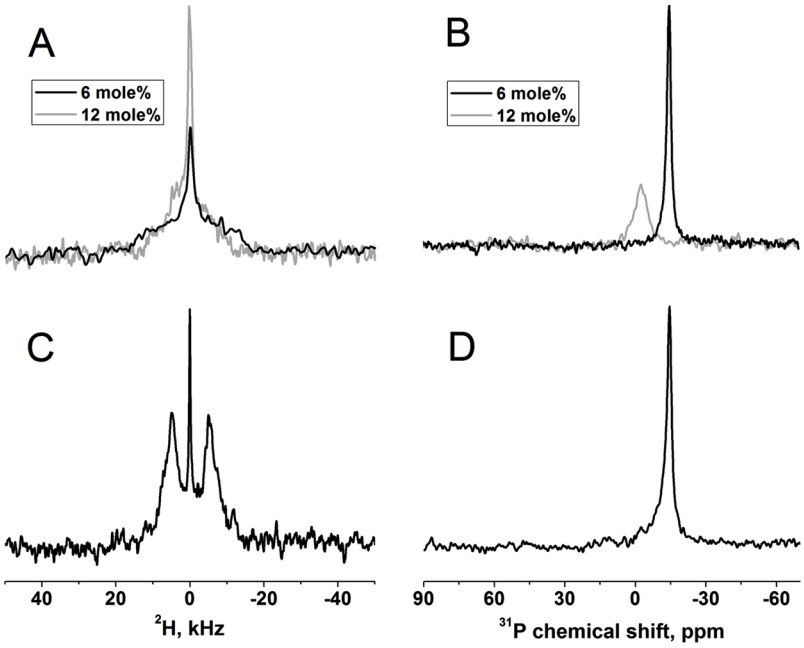

Fig. 2. Solid-state NMR spectra of nanodiscs made of 18A and DMPC.
^{2}H (A, C), and proton-decoupled ^{31}P (B, D) solid-state NMR spectra are shown of nanodiscs that spontaneously orient in the 7 T magnetic field of the NMR spectrometer. The samples are made of [^{15}N-F^{6},^{2}H$_3$-A^{5}]-18A (Ac-DWLKA FYDKV AEKLK EAF- NH2) (A,B) or [^{15}N-V^{10},^{2}H$_3$-A^{11}]-18A (C,D) and DMPC at a peptide-to-lipid ratio of 6 mol% (black lines) or 12 mol% (grey lines). Samples are composed of 4 mg peptide, 20 mg DMPC and 180 µl deuterium-depleted water (black lines) or 4 mg peptide, 10 mg DMPC and 90 µl deuterium-depleted water (grey lines). The isotropic ^{2}H resonances around 0 ppm in A and C are from residual HDO with possible contributions from peptide undergoing fast realignment. Temperature 37 °C. An exponential apodization function of 300 Hz was used in panels A and C, and 100 Hz for B and D.

corresponding Gaussian distributions. Closely related motional regimes have previously been found to describe well the dynamics of amphipathic peptides of related dimensions (e.g. (Michalek et al., 2013)).

3. Results

Two 18A peptides were synthesized by solid-phase peptide synthesis with two different isotopic labeling schemes and reconstituted into DMPC membranes. The sequences were synthesized with a ^{15}N amide and a ^{2}H$_3$ labelled alanine at different positions to obtain a total of four highly complementary orientational constraints (Bechinger et al., 2011). In a first series of experiments the peptide-to-lipid ratio was adjusted to 6 mol% and the lipid-peptide film fully hydrated, inserted into the 7 T magnetic field of the NMR spectrometer (B_o) and investigated at 37 °C (Fig. 2). Notably the samples show a high degree of helicity when investigated by CD spectroscopy (Fig. S2) confirming the initial design of 18A as an amphipathic class A helix mimetic of apolipoprotein A-I (Anantharamaiah and Goldberg, 2015; Anatharamaiah et al., 1985) and previous structural investigations (Venkatachalapathi et al., 1993). Under these conditions the ^{31}P solid-state NMR spectra are characterized by a single resonance around -14.6 ppm (Fig. 2B,D) indicative of bilayers that orient with their normal perpendicular to B_o. When oriented in this manner, a well resolved ^{2}H quadrupolar splitting of 10 kHz is obtained for the ^{2}H$_3$-alanine-11 position with the LWHH is ± 3 kHz (Fig. 2C, Table 2). For the alanine 5 position the distribution of ^{2}H quadrupolar splittings up to 26 kHz was observed (Fig. 2A, Table 2). These values are clearly different from a $\Delta\nu_Q$ = 0 kHz value that would be obtained for a freely moving peptide. Previously it has been shown that for amphipathic peptides the motions in such membrane alignments interfere with efficient ^{1}H-^{15}N cross-polarization (Aisenbrey and Bechinger, 2004a; Salnikov et al., 2018) and this is probably also the case for 18A. Upon further addition of 18A to reach a ratio of 12 mol% the isotropic ^{31}P chemical shift and ^{2}H spectral line shape are indicative of formation of structures that tumble fast in the NMR magnetic field (Fig. 2A,B, grey lines)

In a next step the same 18A/DMPC mixtures were applied onto solid-supports, equilibrated at 93% r.h., the resulting membrane stacks introduced into the NMR spectrometer with the normal parallel to the magnetic field direction and the solid-state spectra recorded (Fig. 3). The ^{31}P solid-state NMR spectra are indicative of well-oriented phosphadidylcholine lipid bilayers in their liquid crystalline state with a predominant peak at 28 ppm (Fig. 3C,F). Some additional intensities spread up to -17 ppm showing that some lipids are not aligned parallel to the sample normal and/or conformational heterogeneity at the level of the phospholipid head group (Scherer and Seelig, 1989). This observation of differently aligned ^{31}P contributions is in-line with the very high concentration of amphipathic peptide and with previous investigations (Salnikov et al., 2018). Comparison of the ^{31}P chemical shifts of the bicellar sample at 14.6 ppm with the 17 ppm resonance observed for the 90° tilted glass-plate supported membrane sample (not shown) indicates that motions of the bicelles introduce a scaling factor of 0.85 comparable to previous observations with related peptide nanodiscs (Salnikov et al., 2018).

The ^{2}H solid-state NMR spectra of Ala^{5} and Ala^{11} exhibit quadrupolar splittings of 26 kHz and 19.5 kHz, respectively (Fig. 3B,E, Table 2). Within experimental error, the value for Ala^{11} is twice the size of the one observed for the magnetically aligned sample (Fig. 2C, Table 2) which is due to the 90°-different alignment of the membrane

Table 2
^{15}N and ^{2}H solid-state NMR data of 18A peptides in oriented membranes.

18A	Preparation method	^{2}H$_3$-Ala5, ^{2}H quadrupolar splitting (kHz)	^{15}N-Phe6, ^{15}N chemical shift (ppm)	^{15}N-Val10, ^{15}N chemical shift (ppm)	^{2}H$_3$-Ala11, ^{2}H quadrupolar splitting (kHz)
1 mole%	Oriented on glass plates	25 ± 1.5	66.5 ± 3	65 ± 3	23.8 ± 1.0
6 mole%		26 ± 2	66 ± 3	66 ± 3	19.5 ± 1.5
6 mole%	magnetically oriented	Isotropic, broad, ≤26			10 ± 3
12 mole%	nanodiscs	Isotropic, broad, ≤20			

± represents the line width at 50% intensity (LWHH). For the mechanically aligned sample the normal is oriented parallel to the magnetic field direction, for the magnetic alignment perpendicular. Temperature 37 °C.

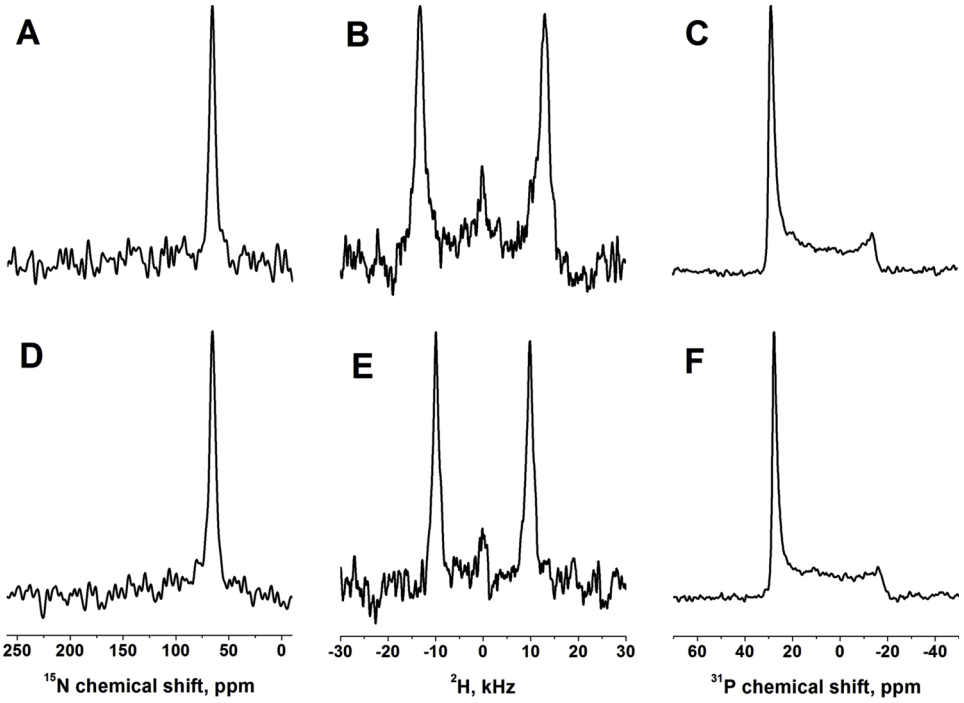

Fig. 3. Solid-state NMR spectra of 6 mol% 18A reconstituted into DMPC membranes mechanically supported on glass plates. Proton-decoupled ^{15}N (A, D), ^{2}H (B, E), and proton-decoupled ^{31}P (C, F) solid-state NMR spectra are shown of nanodiscs made of [^{15}N-F^{6},$^{2}H_3$-A^{5}]-18A (A–C) or [^{15}N-V^{10},$^{2}H_3$-A^{11}]-18A (D–F). The sample normal is inserted into the NMR spectrometer parallel to B_o. Temperature 37 °C.

normal when the two samples are compared to each other. The angle Θ between the membrane normal relative to the magnetic field adds a scaling factor of (3*cos^{2}Θ-1) and thus a -2 -fold difference between the 90° and 0° orientations (Aisenbrey and Bechinger, 2004a; Molugu et al., 2017), where the sign of the quadrupolar splitting remains unknown from the experiments. For Ala^5 in the nanodisc sample a broad distribution is observed (Fig. 2A) indicating that motional averaging around the membrane normal is slow compared to the NMR time scale (10^{-4} sec). The variable orientations of the 18A helices relative to the magnetic field result in the superposition of different quadrupolar splittings and concomitantly broad lines (illustrated in Fig. 1 of (Aisenbrey and Bechinger, 2004a).

When the same samples were investigated by ^{15}N cross-polarization solid-state NMR spectroscopy the ^{15}N chemical shifts are 66 ppm for both the Phe^6 and the Val^{10} positions (Fig. 3A,D, Table 2). Notably the ^{15}N and the ^{2}H solid-state NMR spectra are indicative of well oriented samples where the mosaicity for the peptide alignment is only a few degrees (Aisenbrey and Bechinger, 2004b). In contrast, significant signal intensities in the ^{31}P solid-state NMR spectra demonstrate the presence of different alignments of the lipid head groups (Fig. 3C, F). Thus, it seems that the lipid adjusts to the well-oriented peptide scaffold. The observations of phospholipid spectra exhibiting alignment distributions when at the same time the peptide spectra are well-oriented has been observed previously with other amphipathic sequences (Kim et al., 2009; Verly et al., 2009; Wolf et al., 2017).

In a last step, the 18A sequence was reconstituted into DMPC at a peptide-to-lipid ratio of 1/100, i.e. a concentration below the bilayer-to-bicelle transition (Bechinger, 2005; Salnikov et al., 2018; Sanders and Prosser, 1998; Wolf et al., 2017). Similar ratios have also been used previously for the investigation of the lipid interactions of other amphipathic polypeptides (Fillion and Auger, 2015; Michalek et al., 2013; Naito et al., 2018; Perrin et al., 2015; Sani and Separovic, 2018). All spectra are indicative of an excellent sample alignment on solid supports (Fig. 4). The ^{31}P main intensity occurs at 30 ppm with little additional spread (Fig. 4C, F). The ^{2}H quadrupolar splittings occur at 25 and 23.8 kHz for Ala^5 and Ala^{11}, respectively, and are characterized by a somewhat sharper appearance than at 6 mol% (Figs. 3B,E and 4 B,E, Table 2). Whereas the Ala^5 splitting does not change compared to the 6 mol% sample within experimental error the Ala^{11} site exhibits a 4 kHz increase (Table 2). The ^{15}N solid-state NMR spectra of Phe^6 and Val^{10} exhibit chemical shifts of 66.5 and 65 ppm, respectively, values almost identical with those observed at 6 mol% (Table 2).

Identical ^{15}N chemical shifts and quadrupolar splittings are observed for the two ^{15}N labelled sites and for the $^{2}H_3$-Ala^5 position (Table 2) when the 1 mol% and 6 mol% glass plate samples are compared to each other. However, Ala^{11} exhibits a 19.5 ± 1.5 kHz quadrupolar splitting (Fig. 3E), at 6 mol%, which is 4 kHz smaller than in the 1 mol% mixture. Such a change could represent a topological change or an increase of motional averaging or both upon increase in the peptide-to-lipid ratio, although one would rather expect more restricted dynamics at the higher peptide-to-lipid ratios.

The solid-state NMR orientational restraints contain information to quantitatively analyze the topology of the peptide relative to the magnetic field direction, and thereby the coinciding bilayer normal in the mechanically oriented samples (Figs. 3 and 4, Table 2). The measured solid-state NMR parameters are anisotropic with orientation-dependent values between 55 and 225 ppm for the ^{15}N chemical shift (Salnikov et al., 2009) and methyl quadrupolar splittings between -40 and 80 kHz (Batchelder et al., 1983) and can be used to restrict the number of possible alignments (Bechinger and Sizun, 2003). When the labeled sites are within a single structural domain, the four experimentally determined ^{15}N chemical shifts and quadrupolar splittings can be combined to much restrict its possible membrane topology, possibly to a single alignment that agrees with all the measurements (Aisenbrey et al., 2006; Bechinger et al., 2011; Salnikov et al., 2018). In particular, the ^{15}N and $^{2}H_3$ alanine measurements are highly complementary and can be combined in peptides prepared by chemical synthesis (Bechinger et al., 2011).

A restriction analysis is shown in Fig. 5 where all possible combinations of helical tilt and pitch angles are tested against the experimentally observed values including a range defined by the LWHH (Bechinger and Salnikov, 2012). The topological restraints from each NMR measurement are shown in Fig. 5A and C for ^{15}N-V^{10} in blue, for ^{15}N-F^6 in red, for $^{2}H_3$-A^5 in black, and for $^{2}H_3$-A^{11} in green. The orientational restraints were obtained assuming first a static peptide and second rocking and wobbling motions of the helix by taking into account an 18° and 10° Gaussian distribution, respectively, similar to motions that have been found reasonable for other amphipathic helical

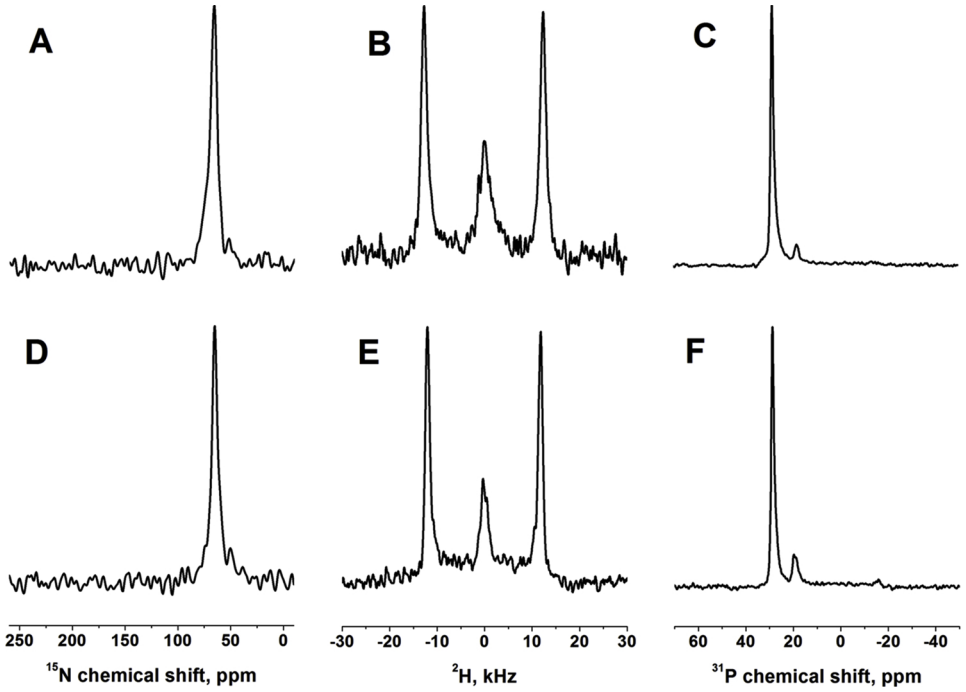

Fig. 4. Solid-state NMR spectra of 1 mol% 18A reconstituted into DMPC membranes mechanically aligned on glass plates. Proton-decoupled ^{15}N (A, D), ^{2}H (B, E), and proton-decoupled ^{31}P (C, F) solid-state NMR spectra are shown of [^{15}N-F^{6},^{2}H$_3$-A^{5}]-18A (A–C) or [^{15}N-V^{10},^{2}H$_3$-A^{11}]-18A (D–F). The small ^{31}P NMR resonance at 18 ppm is probably from lipid degradation that may occur during the extended acquisitions of the peptide spectra shown in panels A,B,D,E. The glass plate normal is parallel to B_o. Temperature 37 °C.

peptides of similar dimensions (Michalek et al., 2013; Salnikov et al., 2018). The overlap of all four restrictions and thus the experimentally determined peptide orientation is highlighted by a yellow circle in Fig. 5A–D and the definitions of the pitch and tilt angles are illustrated in Fig. 5E.

To calculate the helix topology without detailed knowledge of the 18A structure in lipid membranes the restriction analysis was first performed for a helical conformation with Ramachandran angles (φ = -65°, ψ = -45°). With the NMR parameters presented in Table 2 for the peptide-to-lipid ratio of 1% this results in a tilt/pitch angular pair of 90° ± 5° / 89° ± 5° (Fig. 5B, Table 3), i.e. pitch angle values near 90° as expected for the amphipathic properties of the peptide. However, two intersections are obtained for the data obtained from the 6 mol% sample both in the absence or presence of wobbling and rocking motions (Fig. 5C,D, Table 3) leaving some ambiguity. In this case the four restraints intersect at tilt/pitch angular regions 90° ± 5° / 93° ± 5° and at 105° ± 5° / 108° ± 5° when wobbling and rocking motions are taken into account. The first solution is close to the topology obtained for the 1 mol% sample where a 4° shift in the pitch angle correlates with a 4 kHz difference in the quadrupolar splitting of ^{2}H$_3$-Ala^{11}. The second solution much resembles the topology obtained for 14A nanodiscs where a (103° ± 5° / 117° ± 5°) alignment was obtained with similar angle definitions (see (Salnikov et al., 2018)).

In addition, other slightly different structures, all within the region commonly observed for the α-helical region of the Ramachandran plot, were tested (Table 3). For 14A, where data of similar quality were available, the experimental errors in the determination of the tilt and pitch angles were estimated < 5°, but systematic errors of about 10° arise from variations in the ^{15}N tensor parameters (Salnikov et al., 2009) and uncertainties about the motional regime of the peptides in lipid bilayers (Michalek et al., 2013; Salnikov et al., 2018). Here we used wobbling and rocking motions of the helical peptide in liquid crystalline bilayer that have been found suitable to describe the motions of peptides of similar size and amphipathy (Michalek et al., 2013; Salnikov et al., 2018; Strandberg et al., 2009) but static arrangements or smaller excursions could also be feasible to fit the NMR data (Table 3; cf. detailed analysis in (Michalek et al., 2013)).

When previous ^{15}N chemical shift measurements of 18A in POPC (Salnikov et al., 2018) were tested they also fit the topological analysis presented in Fig. 5 and Table 3. Good agreement with the current topologies is obtained although different lipid fatty acyl chains and/or other concentrations were used in these previous experiments (Table 3).

We also tested the effect of incorporating a transmembrane helical polypeptide on the magnetic orientation of bicelles. Solid-state NMR spectra of the DQA1 and DQB1 TMD domains of MHC II in bicelles are shown in Fig. 6. The bicelles interact with the magnetic field (17.6 T) and result in the ^{31}P solid-state NMR shown in Fig. 6B,D. The narrow ^{31}P NMR resonances at -14.5 ppm are indicative of the bilayer portion of the bicelles where the lipid long axes orient with their membrane normal perpendicular to B_o (Fig. 6B,D). An additional resonance at -2 ppm arises from short chain lipids that can adopt a multitude of alignments in fast exchange and which are localized along the rim of the bicelle (Sanders and Schwonek, 1992).

The ^{15}N solid-state NMR spectra of DQA1 labelled at the Gly^{15} position is characterized by a ^{15}N chemical shifts of 87 ± 13 ppm (LWHH) however this signal is rather low despite the extended measuring time of two days (Fig. 6A). When the Leu16 position of DQA1 is labelled with ^{15}N closely related solid-state NMR spectra are obtained (not shown). In comparison, the related sequence [^{15}N-L^{19}]-DQB1 shows a strong intensity at 90 ± 5 ppm (Fig. 6C). The presence of a single resonance (rather than a circular powder pattern like distribution) is indicative of fast rotational averaging around the membrane normal of the helix and/or the bicelle as a whole (Aisenbrey and Bechinger, 2004a).

As an alternative means for membrane extraction and of bicelle formation, SMA copolymers have been used and are continuously developed (Dorr et al., 2014; Knowles et al., 2009; Ravula et al., 2018). Another polymer, DIBMA (Fig. 7D), has been found to be an efficient agent for membrane protein extraction with the additional advantage to be devoid of aromatic groups which interfere with many optical techniques (Oluwole et al., 2017b). Here we tested the magnetic alignment properties of DIBMA-based nanodiscs (Fig. 7). Indeed when 10 mM POPC is mixed with the polymer at a 1:1 wt/wt ratio and introduced into the 17.6 T magnetic field of the NMR spectrometer a sharp ^{31}P solid-state NMR intensity is observed at -12 ppm, indicative of an alignment of the bilayer normal perpendicular to B_o (Fig. 7A). In contrast, when a 100 mM lipid suspension is investigated, i.e. concentrations typically required to observe oriented spectra of bicelle-

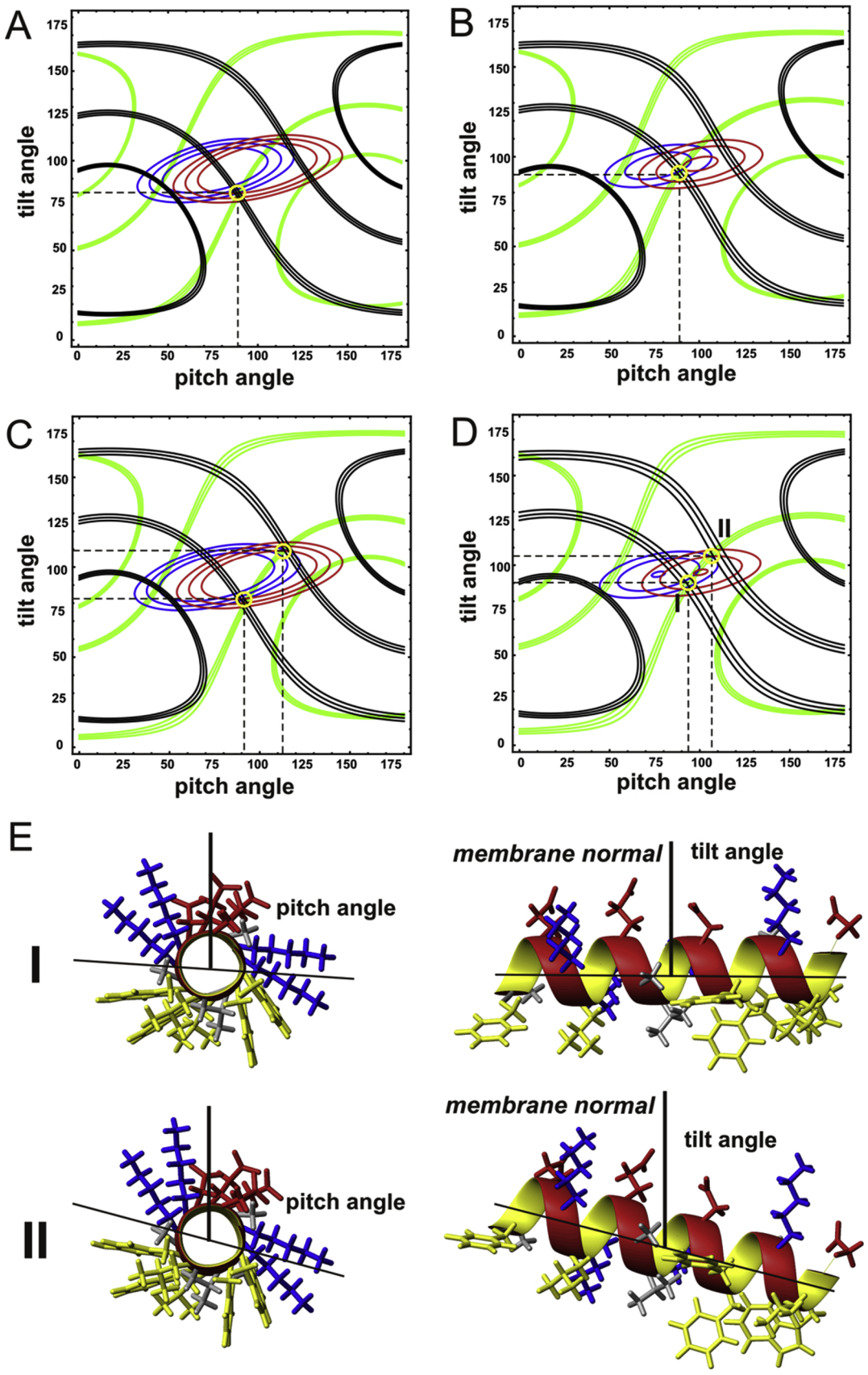

(caption on next page)

Fig. 5. Analysis of NMR topological restraints for 18A reconstituted into mechanically oriented DMPC membranes. Contour plot simulations using the NMR data at 1 mol% 18A (**A** and **B**, data shown in Fig. 4 and Table 2) and at 6 mol% 18A (**C** and **D**, data shown in Fig. 3 and Table 2). The topological restraints from each NMR measurement are shown for ^{15}N-V^{10} in blue, for ^{15}N-F^{6} in red, for ^{2}H$_3$-A^{5} in black, and for ^{2}H$_3$-A^{11} in green. The restraints were obtained assuming either a static peptide alignment (panels **A** and **C**) or rocking and wobbling motions of the helix (panels **B** and **D**, *see* text for details). Whereas, in each case the central line represents the main intensity, two additional restrictions were calculated from values representing the LWHH to take into account orientational distributions as provided in Table 1. The alignment of a peptide with α-helical dihedral angles (φ = -65°, ψ = -45°) and two different topologies from panel D (I: tilt 90°/pitch 93° and II: tilt 105°/pitch 108°) are represented in panel **E.** The pitch angle represents rotations around the helix long axis before the helix is tilted relative to the membrane normal (tilt angle). The amino acid sidechains are shown in the following colours: leucines, phenylalanines, tryptophans and tyrosines in yellow, glutamic and aspartic acid in red, lysines in blue, and alanines and valine in grey.

reconstituted peptides (cf. Fig. 6) partial magnetic alignment is only observed after a freeze/thaw cycle (Fig. 7B,C). Notably, the phospholipid/polymer ratio is 2/1 wt/wt in these samples because an isotropic signal intensity was observed at the higher ratio used for the 10 mM lipid concentration. Whereas the size of the discs is tuned by the lipid-to-polymer ratio (Oluwole et al., 2017b) the absolute concentration also influences the size of the discs and required a readjustment of the size. Addition of the thulium lanthanide flips the corresponding polymer-encapsulated nanodiscs into an alignment with the phospholipid long axis parallel to the magnetic field direction (Fig. 7E,F).

Table 3
Tilt and angular pitch angles from solid-state angular restraints.

Alpha helix	1 mole%		6 mole%	
	static	fluctuations	static	fluctuations
φ = -62°, ψ = -45°	no fit	98° / 80°	no fit	97° / 84°[a]
φ = -65°, ψ = -45°	82° / 89°[a]	90° / 89°[a]	82° / 91° or 109° / 114°	90° / 93°[a] or 105° / 108°[a]
φ = -68°, ψ = -45°	no fit	104° / 104°	no fit	101° / 106°[a]
φ = -58°, ψ = -47°	no fit	no fit	no fit	101° / 90°[a]

The tilt / pitch angular pairs are indicated. The error bars are 5°; *no fit* indicates that the four orientational restraints do not superimpose at a unique topology.

[a] Alignments in 1 mol% DMPC that also fit with previous measurements where ^{15}N chemical shifts of ^{15}N-Ala^{5} 18A (1 mol%) and ^{15}N-Ala^{17} 18A (1.7 mol%) in POPC published in (Salnikov et al., 2018) were compared. The 6 mol% in DMPC data were compared to 3.8 mol% ^{15}N-Ala^{5} 18A and 3.3 mol% ^{15}N-Ala^{17} 18A in POPC (Salnikov et al., 2018).

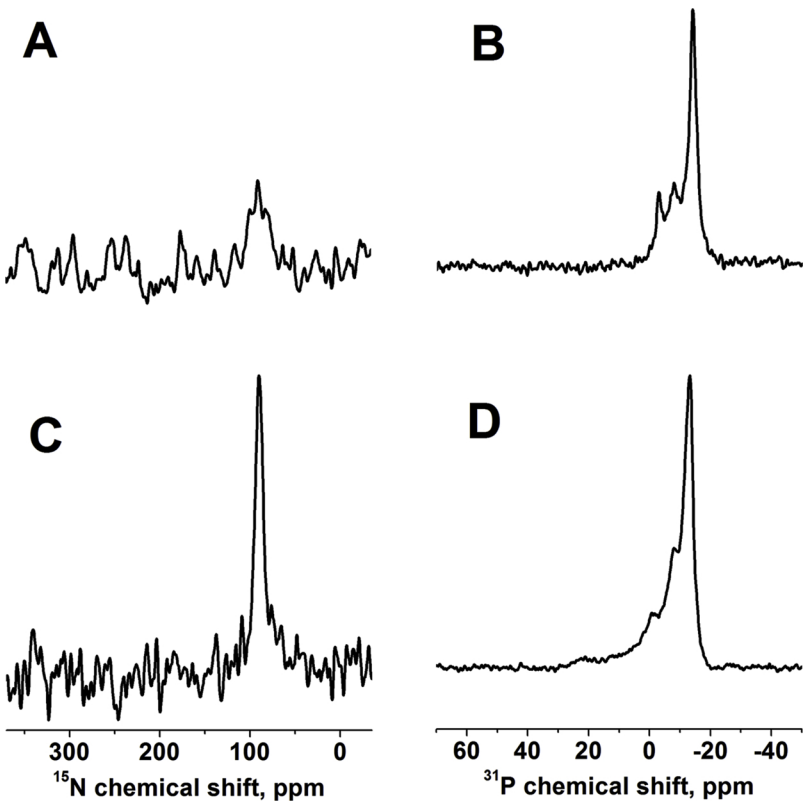

Fig. 6. Solid-state NMR spectra of [^{15}N-G^{15},^{2}H$_3$-A^{9}]-DQA1 (A,B) or [^{15}N-L^{19}]-DQB1 (C,D) reconstituted into DMPC/DHPC bicelles (q = 3.2). Proton-decoupled ^{15}N (A, C) and ^{31}P (B, D) spectra are shown. Temperature 37 °C. The magnetic field is 17.6 T.

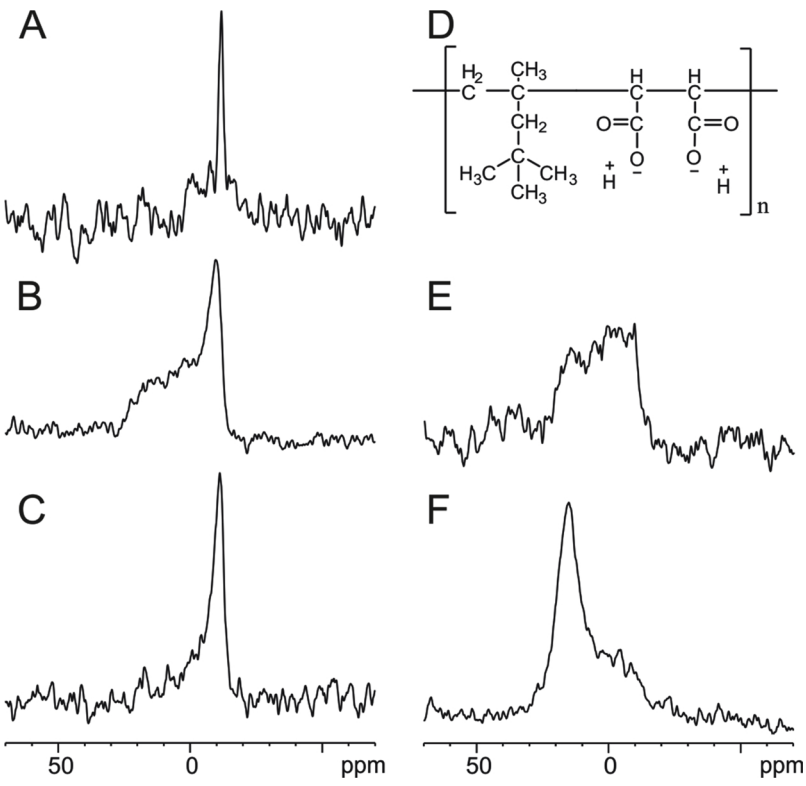

Fig. 7. Proton-decoupled ^{31}P solid-state NMR spectra recorded at 17.6 T of A: 10 mM POPC in the presence of 100 wt% DIBMA at 293 K B: 100 mM POPC in the presence or 50 wt% DIBMA at 293 K C: sample from B at 293 K after cooling to 268 K inside the magnet. D structure of DIBMA, E: 100 mM POPC in the presence of 50 wt% DIBMA and 3 mM $TmCl_3$ at 293 K F: sample from E at 293 K after a cooling cycle to 268 K inside the magnet. All samples are measured in the presence of 10 mM TRIS pH 7.

4. Discussion

4.1. Membrane topology of 18A

The apolipoprotein A-I mimetic peptide 18A was prepared carrying ^{15}N and ^{2}H isotopic labels at selected positions, reconstituted into uniaxially aligned phosphatidylcholine bilayers and investigated by oriented solid-state NMR spectroscopy. The anisotropic ^{15}N chemical shift and the $^{2}H_3$-alanine quadrupolar splittings provide highly complementary angular constraints (Bechinger et al., 2011) that have been analyzed here to yield the detailed membrane topology of the helical peptide. The peptide alignment was investigated at 1 mol% when the peptide partitions into an extended bilayer and at 6 mol% when structures form that align in the magnetic field of the NMR spectrometer. This behavior has been associated with the formation of bicellar discs which are at least 20 nm in diameter (Ravula et al., 2017c; Vold and Prosser, 1996). Indeed, 18A has been shown to form nanostructures (Anatharamaiah et al., 1985), shares homology with 14A, for which the formation of bicelles has been demonstrated ((Salnikov et al., 2018) and references cited therein), and relates to amphipathic antimicrobial peptides which also cause membranes to align in the magnetic field of the NMR spectrometer (Bechinger, 2005; Wolf et al., 2017). Interestingly, despite the profound increase in peptide concentration which is associated with a transition from the bilayer to a bicelle phase, the NMR spectra (cf. Figs. 3 and 4, Table 2) and thereby the conformation and alignment of 18A relative to the bicelle normal hardly changes. Considering the (φ = -65°, ψ = -45°) helical conformation the tilt angle remains constant and at a (close to) parallel alignment along the membrane surface (Table 3, Fig. 5). The pitch angle only changes by a few degrees (Table 3, Fig. 5). This alignment is close to what is expected from estimating the hydrophobic moment of an α-helix encompassing the full 18A sequence (Fig. S1) and in agreement with biophysical investigations of apolipoprotein A-I (Li et al., 2006; Koppaka et al., 1999).

When the 14A and 18A tilt angles are compared to each other, closely related topologies parallel to the membrane surface are observed. Although it is possible to find helix conformations and motional regimes where the tilt angle of both peptides match (e.g. 98° for the 1 mol% samples and 104° for the 6 mol% sample; Table S1) even small changes in the detailed helical conformation or changes in the motional regime result in up to 10° differences for 18A (Table 3) making such a detailed comparison difficult. Furthermore, an ambiguity remains for 18A because two topological intersections are obtained for the bicellar structure. In both cases the transition from the bilayer partitioning at low molar ratios to the bicellar rim at high peptide concentrations is associated with relatively small topological changes (Table 3) considering the very different supramolecular arrangements before and after the phase transition. It seems that screening of the hydrophobic fatty acyl chain and the interactions between the peptides associated with the rim can be achieved by a small additional rotation around the helix long axis, which suggest that the energies involved in the transition are relatively small compared e.g. to an in-plane to transmembrane realignment of helices (Bechinger, 2000; Harmouche and Bechinger, 2018). The pitch angles of 18A are somewhat reduced compared to 14A probably due to 40° larger hydrophilic angle of the first peptide when viewed as a helical wheel (Fig. S1). Furthermore, tryptophans have been shown to serve as an interfacial anchor in membrane proteins, and possibly Trp^2 present at the polar-nonpolar interface of 18A (analogous to the location of Trp in transmembrane proteins) affects the detailed topology of 18A, whereas, it is absent in 14A.

When the dynamics of the deuterated sites of 18A are compared to each other it is striking that the A11 site undergoes rotational averaging when associated with the magnetically oriented nanodisc whereas the A5 site moves on a slower intermediate time scale (Fig. 2A,C). Therefore, local motions at the A11 site have to add to the rotational diffusion of the molecule and bicelle as a whole. Possibly, those motions are restricted for the A5 site. Notably, similar observations have been made for positions 5 and 13 of 14A where the aromatic positions 2 and 6 had been suggested to be involved in intermolecular interactions of helices located in opposing belts (Salnikov et al., 2018).

4.2. Double belt arrangements of these and related complexes involving amphipathic helices

The topologies of 18A and 14A determined here are in line with the suggested head-to-tail double belt arrangements previously suggested for high-density lipoproteins or for nanodiscs formed in the presence of MSP (Gogonea, 2015; Mishra et al., 2006; Schuler et al., 2013) where support comes from a number NMR structural investigations (Bibow et al., 2017; Hagn et al., 2018; Li et al., 2006). A head-to-tail double belt arrangement places the lysines in such a manner to explain the sidedness of their pK values measured by solution-state NMR spectroscopy (Lund-Katz et al., 1995; Mishra et al., 2006). In the double belt arrangement, the hydrophobic fatty acyl chains are shielded from the aqueous environment by a peptide rim.

It is interesting to note that despite the much larger size of apolipoprotein A-I the ^{13}C isotropic chemical shift obtained from MAS solid-state NMR are also in support of the belt model (Li et al., 2006) suggesting that its helices behave as independent units (Mishra et al., 1998) albeit the connecting loops restrict the total circumference of the aggregate without much effect on the individual domains. In this manner 18A provides a suitable model system to better understand the fundamental principles of organization of the more complex apolipoprotein A-I and thereby the high-density lipoprotein complex. For apolipoprotein A-I a number of fluctuating conformations has been observed (Gogonea, 2015; Phillips, 2013) which, upon addition of lipids (Phillips, 2013; White et al., 2014), transform into a much more helical horseshoe shaped fold characterized by a double belt arrangement of helices that are oriented parallel to the bilayer surface. By its reversible membrane association, the protein can adapt to many different environments, similar to the conformational flexibility observed for membrane-active peptides (Bechinger and Aisenbrey, 2012).

4.3. The size and shape of bicelles

Although the size and shape of the 18A-lipid complexes cannot be determined precisely from these solid-state NMR data the magnetic interactions resemble those observed when phosphatidylcholines have been mixed with short chain lipids (Marcotte and Auger, 2005; Nolandt et al., 2012; Prosser et al., 2006; Warschawski et al., 2011), modified lipids (Johansson et al., 2007), amphipathic peptides (Bechinger, 2005; Gogonea, 2015; Handattu et al., 2007; Schuler et al., 2013; Wolf et al., 2017) or SMA copolymers (Ravula et al., 2018). These were associated with the formation of bicelles. Because magnetic alignment is a cooperative process where the magnetic susceptibility anisotropy of a large number of lipid fatty acyl chains has to act in a concerted manner, the supramolecular complexes have to be ≥ 20 nm in diameter (Ravula et al., 2017c; Vold and Prosser, 1996). The exact size of these discs can be tuned by the ratio of rim-forming compounds over long chain phospholipids. Nanodiscs made in the presence of apolipoproteins or the amphipathic helices of the 20–30 kDa membrane scaffolding proteins are typically 10–15 nm in diameter and because of the covalent framework more homogenous in size (Schuler et al., 2013; Warschawski et al., 2011). The latter tumble isotropically in solution and have therefore been developed for multidimensional solution NMR of membrane proteins.

4.4. Magentic alignment of bicelles

The cooperative anisotropy of the magnetic susceptibility associated with the phospholipids drives the alignment of the bicelle normal perpendicular to the magnetic field direction. Here magnetic alignment has been observed in the presence of 18A (Fig. 2) or the DIBMA polymer (Fig. 7). In the latter case, excellent alignment of a 10 mM lipid suspension was spontaneous (Fig. 7A) but needed a freeze/thaw cycle in the magnetic field at 10-times higher concentrations. The temperature changes in this process involves passage through one or several phase transitions from viscous (at ambient temperature) to a more fluid suspension (at low temperature) and probably helps in better mixing and equilibration (Prosser et al., 1998a). These observations suggest that the viscosity of the sample at a high concentration slows down the alignment process (Fig. 7B,C). The size of the DIBMA nanodiscs can be estimated to be > 35 nm where the transition of DMPC from vesicles to DIBMA/DMPC nanodiscs was associated with a very small free energy change (Oluwole et al., 2017b). The orientational preference of the phospholipids can be overcome by lanthanides which flip the alignment of the bilayer normal parallel to B_o (Bechinger et al., 2011; Das et al., 2015; Gopinath et al., 2015; Marcotte and Auger, 2005) and has also been observed here for the DIBMA nanodiscs (Fig. 7F). Notably, although it has been shown that these bicelles can be made to align well in the magnet, the conditions may still need to be optimized for protein NMR samples e.g. by scanning conditions such as temperature, concentration, lipid-to-protein ratio, water content, polymer/lipid ratio etc.

Taken together these and published data, the main role of the rim is to ensure a stable and ordered packing of the phospholipids within an extended bilayer region of the bicelles. In this paper three complementary approaches to form an amphiphilic rim structure are presented. Whereas the investigation of rim-forming peptides that are of significant biomedical importance has allowed us to investigate the structural details of the rim, we also present structural investigations using short chain lipids, a well-established systems to obtain magnetically oriented bicelles, as well as a polymer that has only been introduced recently for such applications. Thus, the polypeptides thereby take the role of short-chain lipids or detergents to shield the hydrophobic fatty acyl chains from the aqueous surroundings. Magnetically aligned phospholipid membranes have also been observed in the presence of other amphipathic peptides such as magainin 2 and derived antimicrobial peptides which form cationic amphipathic helices in the presence of membranes (Bechinger, 2005; Wolf et al., 2017). Furthermore, the melittin peptide from bee venom or the antimicrobial peptide esculentin cause magnetic deformation when interacting with phospholipid vesicles in the magnetic field of NMR spectrometers (Loffredo et al., 2017; Pott and Dufourc, 1995). Notably, bicellar nanodiscs have been used to magnetically orient bilayer-inserted transmembrane domains of other proteins (Das et al., 2015; Gopinath et al., 2015; Ravula et al., 2017c), or of peptides that interact via a myristoyl anchor (Struppe et al., 2000) or by electrostatic interactions (Prosser et al., 1998b), respectively.

Here we also used a lipid bicelle for investigation of the transmembrane domains of DQA1 and DQB1, analogous to previous investigations of other transmembrane proteins (Gopinath et al., 2015; Ravula et al., 2017c). Indeed, the chemical shifts of Gly^{15} and Leu^{16} are indicative of a transmembrane alignment of the DQA1 domain and fast rotational averaging of the peptide and/or the bicelle around the membrane normal (Fig. 6A). The average chemical shift is in agreement with an alignment of the helical domain at about 55° relative to the magnetic field direction (Bechinger and Sizun, 2003; Salnikov et al., 2009). It is also possible that the peptide undergoes wobbling and rocking motions bringing the value closer to the isotropic values of Gly and Leu which are about 108 and 121 ppm for their amide resonances (Salnikov et al., 2009). Notably, it has been observed previously that ^{15}N-amide cross polarization solid-state NMR spectra exhibit reduced intensities when the shifts approach the isotropic value because at these molecular alignments and dynamics the ^{15}N-^{1}H dipolar couplings are small (Raya et al., 2011; Salnikov et al., 2018). This is also an observation made here. Notably, while it was not possible to maintain the bicellar alignment for 70 h of acquisition (not shown), improvements on the sample could provide more efficient acquisition conditions. Because of the 90° angle between the bilayer normal and the magnetic field this data is indicative of a transmembrane helix alignment at a tilt angle of about 35° ± 10°. Similar results are obtained for DQB1 albeit the polypeptide dynamics are more favourable for cross-polarization solid-state NMR (Fig. 6B). The data shown in Fig. 6 are promising first steps in the investigation of the biomedically important MHC-II complex.

Author contributions

ES and CA designed and performed the experiments and analyzed data, GMA helped in writing the paper, BB designed the experiments, helped in the analysis and wrote the paper.

Conflict of interest

It is declared that GMA is a stockowner in Bruin Pharma, a startup biotech company. He is also in the advisory board panel of LipimetiX Ltd, a startup biotech company.

Acknowledgements

We acknowledge Sandro Keller for providing the DIBMA copolymer and for critically reading the manuscript, and Delphine Hatey for her help with peptide synthesis and purification. The discussions with Britta Brügger and Thomas Kupke on DQA1 and its specific sphingomyelin interactions are well appriciated. We are grateful for the financial contributions of the Agence Nationale de la Recherche (projects ProLipIn 10-BLAN-731, membraneDNP 12-BSV5-0012, MemPepSyn 14-CE34-0001-01, InMembrane 15-CE11-0017-01 and the LabEx Chemistry of Complex Systems10-LABX-0026_CSC), the University of Strasbourg, the CNRS, the Région Alsace (Région Grand-Est) and the RTRA International Center of Frontier Research in Chemistry. BB thanks the *Institut Universitaire de France* for providing additional time for research. Work was also partially supported by National Institutes of Health (GM115367, DK108836 and PO1HL128203).

Appendix A. Supplementary data

Supplementary material related to this article can be found, in the online version, at doi:https://doi.org/10.1016/j.chemphyslip.2019.01.012.

References

Aisenbrey, C., Bechinger, B., 2004a. Investigations of peptide rotational diffusion in aligned membranes by 2H and 15N solid-state NMR spectroscopy. J. Am. Chem.Soc. 126, 16676–16683.
Aisenbrey, C., Bechinger, B., 2004b. Tilt and rotational pitch angles of membrane-inserted polypeptides from combined 15N and 2H solid-state NMR spectroscopy. Biochemistry-US 43, 10502–10512.
Aisenbrey, C., Sizun, C., Koch, J., Herget, M., Abele, U., Bechinger, B., Tampe, R., 2006. Structure and dynamics of membrane-associated ICP47, a viral inhibitor of the MHC I antigen-processing machinery. J. Biol. Chem. 281, 30365–30372.
Aisenbrey, C., Michalek, M., Salnikov, E.S., Bechinger, B., 2013. Solid-state NMR approaches to study protein structure and protein-lipid interactions. In: Kleinschmidt, J.H. (Ed.), Lipid-Protein Interactions: Methods and Protocols. Springer, New York, pp. 357–387.
Anantharamaiah, G.M., 1986. Synthetic peptide analogs of apolipoproteins. Methods Enzymol. 128, 627–647.
Anantharamaiah, G.M., Jones, J.L., Brouillette, C.G., Schmidt, C.F., Chung, B.H., Hughes, T.A., Bhown, A.S., Segrest, J.P., 1985. Studies of synthetic peptide analogs of the amphipathic helix. Structure of complexes with dimyristoyl phosphatidylcholine. J. Biol. Chem. 260, 10248–10255.
Anantharamaiah, G.M., Mishra, V.K., Garber, D.W., Datta, G., Handattu, S.P., Palgunachari, M.N., Chaddha, M., Navab, M., Reddy, S.T., Segrest, J.P., Fogelman, A.M., 2007. Structural requirements for antioxidative and anti-inflammatory properties of apolipoprotein A-I mimetic peptides. J. Lipid Res. 48, 1915–1923.
Anantharamaiah, G.M., Goldberg, D. (Eds.), 2015. Apolipoprotein Mimetics in the Management of Human Diseases. ADIS, Springer International Publishing, Switzerland.
Anatharamaiah, G.M., Jones, J.L., Brouillette, C.G., Schmidt, C.F., Chung, B.H., Hughes, T.A., Bhown, A.S., Segrest, J.P., 1985. Studies of synthetic peptide analogs of the amphiphatic helix (structure of complexes with dimyristoyl phosphatidylcholine). J. Biol. Chem. 260, 10248–10255.
Ashby, D.T., Rye, K.A., Clay, M.A., Vadas, M.A., Gamble, J.R., Barter, P.J., 1998. Factors influencing the ability of HDL to inhibit expression of vascular cell adhesion molecule-1 in endothelial cells. Arterioscler. Thromb. Vasc. Biol. 18, 1450–1455.
Assmann, G., Gotto Jr, A.M., 2004. HDL cholesterol and protective factors in atherosclerosis. Circulation 109, III8–III14.
Baker, L.A., Baldus, M., 2014. Characterization of membrane protein function by solid-state NMR spectroscopy. Curr. Opin. Struct. Biol. 27, 48–55.
Batchelder, L.S., Niu, H., Torchia, D.A., 1983. Methyl reorientation in polycrystalline amino acids and peptides: a 2H NMR spin lattice relaxation study. J. Am. Chem. Soc. 105, 2228–2231.
Bechinger, B., 2000. Understanding peptide interactions with lipid bilayers: a guide to membrane protein engeneering. Curr. Opin. Chem. Biol. 4, 639–644.
Bechinger, B., 2005. Detergent-like properties of magainin antibiotic peptides: a 31P solid-state NMR study. Biochim. Biophys. Acta 1712, 101–108.
Bechinger, B., Aisenbrey, C., 2012. The polymorphic nature of membrane-active peptides from biophysical and structural investigations. Curr. Protein Pept. Sci. 13, 602–610.
Bechinger, B., Opella, S.J., 1991. Flat-coil probe for NMR spectroscopy of oriented membrane samples. J. Magn. Reson. 95, 585–588.
Bechinger, B., Salnikov, E.S., 2012. The membrane interactions of antimicrobial peptides revealed by solid-state NMR spectroscopy. Chem. Phys. Lipids 165, 282–301.
Bechinger, B., Resende, J.M., Aisenbrey, C., 2011. The structural and topological analysis of membrane-associated polypeptides by oriented solid-state NMR spectroscopy: established concepts and novel developments. Biophys. Chem. 153, 115–125.
Bechinger, B., Sizun, C., 2003. Alignment and structural analysis of membrane polypeptides by 15N and 31P solid-state NMR spectroscopy. Concepts Magn. Reson. 18A, 130–145.
Bersch, B., Dorr, J.M., Hessel, A., Killian, J.A., Schanda, P., 2017. Proton-detected solid-state NMR spectroscopy of a zinc diffusion facilitator protein in native nanodiscs. Angew. Chem. Int. Ed. Engl. 56, 2508–2512.
Bertani, P., Raya, J., Bechinger, B., 2014. 15N chemical shift referencing in solid state NMR. Solid State Nucl. Magn. Reson. 61–62, 15–18.
Bibow, S., Polyhach, Y., Eichmann, C., Chi, C.N., Kowal, J., Albiez, S., McLeod, R.A., Stahlberg, H., Jeschke, G., Guntert, P., Riek, R., 2017. Solution structure of discoidal high-density lipoprotein particles with a shortened apolipoprotein A-I. Nat. Struct. Mol. Biol. 24, 187–193.
Bjorkholm, P., Ernst, A.M., Hacke, M., Wieland, F., Brugger, B., von Heijne, G., 2014. Identification of novel sphingolipid-binding motifs in mammalian membrane proteins. Biochim. Biophys. Acta 1838, 2066–2070.
Cockerill, G.W., Huehns, T.Y., Weerasinghe, A., Stocker, C., Lerch, P.G., Miller, N.E., Haskard, D.O., 2001. Elevation of plasma high-density lipoprotein concentration reduces interleukin-1-induced expression of E-selectin in an in vivo model of acute inflammation. Circulation 103, 108–112.
Contreras, F.X., Ernst, A.M., Haberkant, P., Bjorkholm, P., Lindahl, E., Gonen, B., Tischer, C., Elofsson, A., von Heijne, G., Thiele, C., Pepperkok, R., Wieland, F., Brugger, B., 2012. Molecular recognition of a single sphingolipid species by a protein's transmembrane domain. Nature 481, 525–529.
Das, N., Dai, J., Hung, I., Rajagopalan, M.R., Zhou, H.X., Cross, T.A., 2015. Structure of CrgA, a cell division structural and regulatory protein from Mycobacterium tuberculosis, in lipid bilayers. Proc. Natl. Acad. Sci. U. S. A. 112, E119–126.
Davis, J.H., Jeffrey, K.R., Bloom, M., Valic, M.I., Higgs, T.P., 1976. Quadrupolar echo deuteron magnetic resonance spectroscopy in ordered hydrocarbon chains. Chem. Phys. Lett. 42, 390–394.
Dorr, J.M., Koorengevel, M.C., Schafer, M., Prokofyev, A.V., Scheidelaar, S., van der Cruijsen, E.A., Dafforn, T.R., Baldus, M., Killian, J.A., 2014. Detergent-free isolation, characterization, and functional reconstitution of a tetrameric K+ channel: the power of native nanodiscs. Proc. Natl. Acad. Sci. U. S. A. 111, 18607–18612.
Dunbar, R.L., Movva, R., Bloedon, L.T., Duffy, D., Norris, R.B., Navab, M., Fogelman, A.M., Rader, D.J., 2017. Oral apolipoprotein A-I mimetic D-4F lowers HDL-Inflammatory index in high-risk patients: a first-in-Human multiple-dose, randomized controlled trial. Clin. Transl. Sci. 10, 455–469.
Durr, U.H.N., Gildenberg, M., Ramamoorthy, A., 2012. The magic of bicelles lights up membrane protein structure. Chem. Rev. 112, 6054–6074.
Eddy, M.T., Su, Y., Silvers, R., Andreas, L., Clark, L., Wagner, G., Pintacuda, G., Emsley, L., Griffin, R.G., 2015. Lipid bilayer-bound conformation of an integral membrane beta barrel protein by multidimensional MAS NMR. J. Biomol. NMR 61, 299–310.
Epand, R.M., Gawish, A., Iqbal, M., Gupta, K.B., Chen, C.H., Segrest, J.P., Anantharamaiah, G.M., 1987. Studies of synthetic peptide analogs of the amphipathic helix. Effect of charge distribution, hydrophobicity, and secondary structure on lipid association and lecithin:cholesterol acyltransferase activation. J. Biol. Chem. 262, 9389–9396.
Fiaux, J., Bertelsen, E.B., Horwich, A.L., Wuthrich, K., 2002. NMR analysis of a 900K GroEL GroES complex. Nature 418, 207–211.
Fillion, M., Auger, M., 2015. Oriented samples: a tool for determining the membrane topology and the mechanism of action of cationic antimicrobial peptides by solid-state NMR. Biophys. Rev. 7, 311–320.
Frey, L., Lakomek, N.A., Riek, R., Bibow, S., 2017. Micelles, Bicelles, and nanodiscs: comparing the impact of membrane mimetics on membrane protein backbone dynamics. Angew. Chem. Int. Ed. Engl. 56, 380–383.
Fung, B.M., Khitrin, A.K., Ermolaev, K., 2000. An improved broadband decoupling sequence for liquid crystals and solids. J. Magn. Reson. 142, 97–101.
Gogonea, V., 2015. Structural insights into high density lipoprotein: old models and new facts. Front. Pharmacol. 6, 318.
Gopinath, T., Mote, K.R., Veglia, G., 2015. Simultaneous acquisition of 2D and 3D solid-state NMR experiments for sequential assignment of oriented membrane protein samples. J. Biomol. NMR 62, 53–61.
Hagn, F., Nasr, M.L., Wagner, G., 2018. Assembly of phospholipid nanodiscs of controlled size for structural studies of membrane proteins by NMR. Nat. Protoc. 13, 79–98.
Handattu, S.P., Garber, D.W., Horn, D.C., Hughes, D.W., Berno, B., Bain, A.D., Mishra, V.K., Palgunachari, M.N., Datta, G., Anantharamaiah, G.M., Epand, R.M., 2007. ApoA-I mimetic peptides with differing ability to inhibit atherosclerosis also exhibit differences in their interactions with membrane bilayers. J. Biol. Chem. 282, 1980–1988.
Harmouche, N., Bechinger, B., 2018. Lipid-mediated interactions between the

amphipathic antimicrobial peptides magainin 2 and PGLa in phospholipid bilayers. Biophys. J. 115, 1033–1044.
Hediger, S., Meier, B.H., Kurur, N.D., Bodenhausen, G., Ernst, R.R., 1994. NMR cross-polarization by adiabatic passage through the Hartmann-Hahn condition (APHH). Chem. Phys. Lett. 223, 283–288.
Johansson, E., Lundquist, A., Zuo, S., Edwards, K., 2007. Nanosized bilayer disks: attractive model membranes for drug partition studies. Biochim. Biophys. Acta 1768, 1518–1525.
Jorgensen, E.V., Anantharamaiah, G.M., Segrest, J.P., Gwynne, J.T., Handwerger, S., 1989. Synthetic amphipathic peptides resembling apolipoproteins stimulate the release of human placental lactogen. J. Biol. Chem. 264, 9215–9219.
Kaul, S., Coin, B., Hedayiti, A., Yano, J., Cercek, B., Chyu, K.Y., Shah, P.K., 2004. Rapid reversal of endothelial dysfunction in hypercholesterolemic apolipoprotein E-null mice by recombinant apolipoprotein A-I(Milano)-phospholipid complex. J. Am. Coll. Cardiol. 44, 1311–1319.
Kim, C., Spano, J., Park, E.K., Wi, S., 2009. Evidence of pores and thinned lipid bilayers induced in oriented lipid membranes interacting with the antimicrobial peptides, magainin-2 and aurein-3.3. Biochim. Biophys. Acta 1788, 1482–1496.
Kim, J., Masterson, L.R., Cembran, A., Verardi, R., Shi, L., Gao, J., Taylor, S.S., Veglia, G., 2015. Dysfunctional conformational dynamics of protein kinase A induced by a lethal mutant of phospholamban hinder phosphorylation. Proc. Natl. Acad. Sci. U. S. A. 112, 3716–3721.
Knowles, T.J., Finka, R., Smith, C., Lin, Y.P., Dafforn, T., Overduin, M., 2009. Membrane proteins solubilized intact in lipid containing nanoparticles bounded by styrene maleic acid copolymer. J. Am. Chem. Soc. 131, 7484–7485.
Kontush, A., Chapman, M.J., 2006. Functionally defective high-density lipoprotein: a new therapeutic target at the crossroads of dyslipidemia, inflammation, and atherosclerosis. Pharmacol. Rev. 58, 342–374.
Koppaka, V., Silvestro, L., Engler, J.A., Brouillette, C.G., Axelsen, P.H., 1999. The structure of human lipoprotein A-I. Evidence for the "belt" model. J. Biol. Chem. 274, 14541–14544.
Ladizhansky, V., 2017. Applications of solid-state NMR to membrane proteins. Biochim. Biophys. Acta 1865, 1577–1586.
Lakomek, N.A., Frey, L., Bibow, S., Bockmann, A., Riek, R., Meier, B.H., 2017. Proton-detected NMR spectroscopy of nanodisc-embedded membrane proteins: MAS solid-state vs solution-state methods. J. Phys. Chem. B 121, 7671–7680.
Lalli, D., Idso, M.N., Andreas, L.B., Hussain, S., Baxter, N., Han, S., Chmelka, B.F., Pintacuda, G., 2017. Proton-based structural analysis of a heptahelical transmembrane protein in lipid bilayers. J. Am. Chem. Soc. 139, 13006–13012.
Li, Y., Kijac, A.Z., Sligar, S.G., Rienstra, C.M., 2006. Structural analysis of nanoscale self-assembled discoidal lipid bilayers by solid-state NMR spectroscopy. Biophys.J. 91, 3819–3828.
Loffredo, M.R., Ghosh, A., Harmouche, N., Casciaro, B., Luca, V., Bortolotti, A., Cappiello, F., Stella, L., Bhunia, A., Bechinger, B., Mangoni, M.L., 2017. Membrane perturbing activities and structural properties of the frog-skin derived peptide Esculentin-1a(1-21)NH2 and its Diastereomer Esc(1-21)-1c: correlation with their antipseudomonal and cytotoxic activity. Biochim. Biophys. Acta 1859, 2327–2339.
Loudet, C., Diller, A., Grelard, A., Oda, R., Dufourc, E.J., 2010. Biphenyl phosphatidylcholine: a promoter of liposome deformation and bicelle collective orientation by magnetic fields. Prog. Lipid Res. 49, 289–297.
Lund-Katz, S., Phillips, M.C., Mishra, V.K., Segrest, J.P., Anantharamaiah, G.M., 1995. Microenvironments of basic amino acids in amphipathic alpha-helices bound to phospholipid: 13C NMR studies using selectively labeled peptides. Biochemistry-US 34, 9219–9226.
Marcotte, I., Auger, M., 2005. Bicelles as model membranes for solid- and solution-state NMR studies of membrane peptides and proteins. Concepts Magn. Reson. Part A 24A, 17–37.
Michalek, M., Salnikov, E., Werten, S., Bechinger, B., 2013. Structure and topology of the huntingtin 1-17 membrane anchor by a combined solution and solid-state NMR approach. Biophys. J. 105, 699–710.
Mishra, V.K., Palgunachari, M.N., Datta, G., Phillips, M.C., Lund-Katz, S., Adeyeye, S.O., Segrest, J.P., Anantharamaiah, G.M., 1998. Studies of synthetic peptides of human apolipoprotein A-I containing tandem amphipathic alpha-helixes. Biochemistry-US 37, 10313–10324.
Mishra, V.K., Anantharamaiah, G.M., Segrest, J.P., Palgunachari, M.N., Chaddha, M., Sham, S.W., Krishna, N.R., 2006. Association of a model class A (apolipoprotein) amphipathic alpha helical peptide with lipid: high resolution NMR studies of peptide.lIpid discoidal complexes. J. Biol. Chem. 281, 6511–6519.
Molugu, T.R., Lee, S., Brown, M.F., 2017. Concepts and methods of solid-state NMR spectroscopy applied to biomembranes. Chem. Rev. 117, 12087–12132.
Naito, A., Matsumori, N., Ramamoorthy, A., 2018. Dynamic membrane interactions of antibacterial and antifungal biomolecules, and amyloid peptides, revealed by solid-state NMR spectroscopy. Biochim. Biophys. Acta 1862, 307–323.
Navab, M., Anantharamaiah, G.M., Hama, S., Garber, D.W., Chaddha, M., Hough, G., Lallone, R., Fogelman, A.M., 2002. Oral administration of an Apo A-I mimetic Peptide synthesized from D-amino acids dramatically reduces atherosclerosis in mice independent of plasma cholesterol. Circulation 105, 290–292.
Navab, M., Anantharamaiah, G.M., Reddy, S.T., Hama, S., Hough, G., Grijalva, V.R., Wagner, A.C., Frank, J.S., Datta, G., Garber, D., Fogelman, A.M., 2004. Oral D-4F causes formation of pre-beta high-density lipoprotein and improves high-density lipoprotein-mediated cholesterol efflux and reverse cholesterol transport from macrophages in apolipoprotein E-null mice. Circulation 109, 3215–3220.
Newton, R.S., Krause, B.R., 2002. HDL therapy for the acute treatment of atherosclerosis. Atheroscler. Suppl. 3, 31–38.
Nissen, S.E., Tsunoda, T., Tuzcu, E.M., Schoenhagen, P., Cooper, C.J., Yasin, M., Eaton, G.M., Lauer, M.A., Sheldon, W.S., Grines, C.L., Halpern, S., Crowe, T., Blankenship, J.C., Kerensky, R., 2003. Effect of recombinant ApoA-I Milano on coronary atherosclerosis in patients with acute coronary syndromes: a randomized controlled trial. JAMA 290, 2292–2300.
Nolandt, O.V., Walther, T.H., Grage, S.L., Ulrich, A.S., 2012. Magnetically oriented dodecylphosphocholine bicelles for solid-state NMR structure analysis. BBA-Biomembranes 1818, 1142–1147.
Oluwole, A.O., Danielczak, B., Meister, A., Babalola, J.O., Vargas, C., Keller, S., 2017a. Solubilization of membrane proteins into functional lipid-bilayer nanodiscs using a diisobutylene/maleic acid copolymer. Angew. Chem. Int. Ed. Engl. 56, 1919–1924.
Oluwole, A.O., Klingler, J., Danielczak, B., Babalola, J.O., Vargas, C., Pabst, G., Keller, S., 2017b. Formation of lipid-bilayer nanodiscs by diisobutylene/maleic acid (DIBMA) copolymer. Langmuir 33, 14378–14388.
Park, S.H., Berkamp, S., Cook, G.A., Chan, M.K., Viadiu, H., Opella, S.J., 2011. Nanodiscs versus macrodiscs for NMR of membrane proteins. Biochemistry-US 50, 8983–8985.
Perrin Jr, B.S., Sodt, A.J., Cotten, M.L., Pastor, R.W., 2015. The curvature induction of surface-bound antimicrobial peptides piscidin 1 and piscidin 3 varies with lipid chain length. J. Membr. Biol. 248, 455–467.
Phillips, M.C., 2013. New insights into the determination of HDL structure by apolipoproteins: thematic review series: high density lipoprotein structure, function, and metabolism. J. Lipid Res. 54, 2034–2048.
Pott, T., Dufourc, E.J., 1995. Action of melittin on the DPPC-cholesterol liquid-ordered phase: a solid state 2 H-and 3 1 P-NMR study. Biophys. J. 68, 965–977.
Prosser, R.S., Hwang, J.S., Vold, R.R., 1998a. Magnetically aligned phospholipid bilayers with positive ordering: a new model membrane system. Biophys. J. 74, 2405–2418.
Prosser, R.S., Volkov, V.B., Shiyanovskaya, I.V., 1998b. Novel chelate-induced magnetic alignment of biological membranes. Biophys. J. 75, 2163–2169.
Prosser, R.S., Evanics, F., Kitevski, J.L., Al-Abdul-Wahid, M.S., 2006. Current applications of bicelles in NMR studies of membrane-associated amphiphiles and proteins. Biochemistry-US 45, 8453–8465.
Radoicic, J., Park, S.H., Opella, S.J., 2018. Macrodiscs comprising SMALPs for oriented sample solid-state NMR spectroscopy of membrane proteins. Biophys. J. 115, 22–25.
Ramadugu, V.S.K., Di Mauro, G.M., Ravula, T., Ramamoorthy, A., 2017. Polymer nanodiscs and macro-nanodiscs of a varying lipid composition. Chem. Commun. (Camb.) 53, 10824–10826.
Rance, M., Byrd, R.A., 1983. Obtaining high-fidelity spin-1/2 powder spectra in anisotropic media: phase-cycled hahn echo spectroscopy. J. Magn. Reson. 52, 221–240.
Ravula, T., Barnaba, C., Mahajan, M., Anantharamaiah, G.M., Im, S.C., Waskell, L., Ramamoorthy, A., 2017a. Membrane environment drives cytochrome P450's spin transition and its interaction with cytochrome b5. Chem. Commun. (Camb.) 53, 12798–12801.
Ravula, T., Hardin, N.Z., Ramadugu, S., Cox, S.J., Ramamoorthy, A., 2017b. pH resistant monodispersed polymer-lipid nanodiscs. Angew. Chem. Int. Ed. Engl.
Ravula, T., Ramadugu, S.K., Di Mauro, G., Ramamoorthy, A., 2017c. Bioinspired, size-tunable self-assembly of polymer-lipid bilayer nanodiscs. Angew. Chem. Int. Ed. Engl. 56, 11466–11470.
Ravula, T., Hardin, N.Z., Ramadugu, S.K., Cox, S.J., Ramamoorthy, A., 2018. Formation of pH-resistant monodispersed polymer-lipid nanodiscs. Angew. Chem. Int. Ed. Engl. 57, 1342–1345.
Raya, J., Perrone, B., Bechinger, B., Hirschinger, J., 2011. Chemical shift powder spectra obtained by using ROtor-Directed Exchange of Orientations Cross-Polarization (RODEO-CP). Chem. Phys. Lett. 508, 155–164.
Retel, J.S., Nieuwkoop, A.J., Hiller, M., Higman, V.A., Barbet-Massin, E., Stanek, J., Andreas, L.B., Franks, W.T., van Rossum, B.J., Vinothkumar, K.R., Handel, L., de Palma, G.G., Bardiaux, B., Pintacuda, G., Emsley, L., Kuhlbrandt, W., Oschkinat, H., 2017. Structure of outer membrane protein G in lipid bilayers. Nat. Commun. 8, 2073.
Rubin, E.M., Krauss, R.M., Spangler, E.A., Verstuyft, J.G., Clift, S.M., 1991. Inhibition of early atherogenesis in transgenic mice by human apolipoprotein AI. Nature 353, 265–267.
Russ, W.P., Engelman, D.M., 2000. The GxxxG motif: a framework for transmembrane helix-helix association. J. Mol. Biol. 296, 911–919.
Salnikov, E., Bertani, P., Raap, J., Bechinger, B., 2009. Analysis of the amide (15)N chemical shift tensor of the C(alpha) tetrasubstituted constituent of membrane-active peptaibols, the alpha-aminoisobutyric acid residue, compared to those of di- and trisubstituted proteinogenic amino acid residues. J. Biomol. NMR 45, 373–387.
Salnikov, E.S., Anantharamaiah, G.M., Bechinger, B., 2018. Supramolecular organization of apolipoprotein-A-I-derived peptides within disc-like arrangements. Biophys. J. 115, 467–477.
Sanders, C.R., Prosser, R.S., 1998. Bicelles – a model membrane system for all seasons. Structure 6, 1227–1234.
Sanders, C.R., Schwonek, J.P., 1992. Characterization of magnetically orientable bilayers in mixtures of dihexanoylphosphatidylcholine and dimyristoylphosphatidylcholine by solid-state NMR. Biochemistry-US 31, 8898–8905.
Sani, M.A., Separovic, F., 2018. Antimicrobial peptide structures: from model membranes to live cells. Chemistry 24, 286–291.
Scherer, P.G., Seelig, J., 1989. Electric charge effects on phospholipid headgroups. Phosphatidycholine in mixtures with cationic and anionic amphiphiles. Biochemistry-US 28, 7720–7727.
Schuler, M.A., I.G., D, Sligar, S.G., 2013. Nanodiscs as a new tool to examine lipid-protein interactions. In: Kleinschmidt, J.H. (Ed.), Lipid-Protein Interactions: Methods and Protocols. Springer, New York, pp. 415–433.
Segrest, J.P., Jackson, R.L., Morrisett, J.D., Gotto Jr, M., 1974. A molecular theory of lipid-protein interactions in the plasma lipoproteins. FEBS Lett. 38, 247–253.
Strandberg, E., Esteban-Martin, S., Salgado, J., Ulrich, A.S., 2009. Orientation and dynamics of peptides in membranes calculated from 2H-NMR data. Biophys. J. 96, 3223–3232.

Struppe, J., Whiles, J.A., Vold, R.R., 2000. Acidic phospholipid bicelles: a versatile model membrane system. Biophys. J. 78, 281–289.
Tsai, S., Santamaria, P., 2013. MHC class II polymorphisms, autoreactive T-cells, and autoimmunity. Front. Immunol. 4, 321.
Venkatachalapathi, Y.V., Phillips, M.C., Epand, R.M., Epand, R.F., Tytler, E.M., Segrest, J.P., Anantharamaiah, G.M., 1993. Effect of end group blockage on the properties of a class A amphipathic helical peptide. Proteins 15, 349–359.
Verly, R.M., de Moraes, C.M., Resende, J.M., Aisenbrey, C., Bemquemer, M.P., Pilo-Veloso, D., Valente, A.P., Alemida, F.C., Bechinger, B., 2009. Structure and membrane interactions of the antibiotic peptide dermadistinctin k by solution and oriented 15 N and 31 P solid-state NMR spectroscopy. Biophys. J. 96, 2194–2203.
Vold, R.R., Prosser, R.S., 1996. Magnetically oriented phospholipid bilayered micelles for structural studies of polypeptides – does the ideal bicelle exist. J. Magn. Reson. Ser. B 113, 267–271.
Wang, S., Gopinath, T., Veglia, G., 2018. Application of paramagnetic relaxation enhancements to accelerate the acquisition of 2D and 3D solid-state NMR spectra of oriented membrane proteins. Methods 138–139, 54–61.
Warschawski, D.E., Arnold, A.A., Beaugrand, M., Gravel, A., Chartrand, E., Marcotte, I., 2011. Choosing membrane mimetics for NMR structural studies of transmembrane proteins. Biochim. Biophys. Acta 1808, 1957–1974.
White, C.R., Garber, D.W., Anantharamaiah, G.M., 2014. Anti-inflammatory and cholesterol-reducing properties of apolipoprotein mimetics: a review. J. Lipid Res. 55, 2007–2021.
Wolf, J., Aisenbrey, C., Harmouche, N., Raya, J., Bertani, P., Voievoda, N., Süss, R., Bechinger, B., 2017. pH-dependent membrane interactions of the histidine-rich cell penetrating peptide LAH4-L1. Biophys. J. 113, 1290–1300.
Xu, J., Soong, R., Im, S.C., Waskell, L., Ramamoorthy, A., 2010. INEPT-based separated-local-field NMR spectroscopy: a unique approach to elucidate side-chain dynamics of membrane-associated proteins. J. Am. Chem. Soc. 132, 9944–9947.
Zhang, M., Huang, R., Ackermann, R., Im, S.C., Waskell, L., Schwendeman, A., Ramamoorthy, A., 2016. Reconstitution of the Cytb5 -CytP450 complex in nanodiscs for structural studies using NMR spectroscopy. Angew. Chem. Int. Ed. Engl. 55, 4497–4499.